J. Fluid Mech. (2019), *vol.* 862, *pp.* 449–489. © Cambridge University Press 2019
doi:10.1017/jfm.2018.895

A Lagrangian probability-density-function model for collisional turbulent fluid–particle flows

A. Innocenti[1,2], R. O. Fox[3], M. V. Salvetti[2] and S. Chibbaro[1,†]

[1]Sorbonne Université, Centre National de la Recherche Scientifique, UMR 7190, Institut Jean Le Rond D'Alembert, F-75005 Paris, France

[2]Dipartimento di Ingegneria Civile e Industriale, Università di Pisa, Via G. Caruso 8, 56122 Pisa, Italy

[3]Department of Chemical and Biological Engineering, 618 Bissell Road, Iowa State University, Ames, IA 50011-1098, USA

(Received 2 March 2018; revised 21 September 2018; accepted 6 November 2018; first published online 11 January 2019)

Inertial particles in turbulent flows are characterised by preferential concentration and segregation and, at sufficient mass loading, dense particle clusters may spontaneously arise due to momentum coupling between the phases. These clusters, in turn, can generate and sustain turbulence in the fluid phase, which we refer to as cluster-induced turbulence (CIT). In the present work, we tackle the problem of developing a framework for the stochastic modelling of moderately dense particle-laden flows, based on a Lagrangian probability-density-function formalism. This framework includes the Eulerian approach, and hence can be useful also for the development of two-fluid models. A rigorous formalism and a general model have been put forward focusing, in particular, on the two ingredients that are key in moderately dense flows, namely, two-way coupling in the carrier phase, and the decomposition of the particle-phase velocity into its spatially correlated and uncorrelated components. Specifically, this last contribution allows us to identify in the stochastic model the contributions due to the correlated fluctuating energy and to the granular temperature of the particle phase, which determine the time scale for particle–particle collisions. The model is then validated and assessed against direct-numerical-simulation data for homogeneous configurations of increasing difficulty: (i) homogeneous isotropic turbulence, (ii) decaying and shear turbulence and (iii) CIT.

Key words: multiphase flow, particle/fluid flow, turbulence modelling

1. Introduction

Particle-laden flows represent an important class of natural and industrial flows (Crowe *et al.* 2011). In many applications, these flows are heavily loaded with particles (Stickel & Powell 2005; Forterre & Pouliquen 2008; Guazzelli & Morris 2011) and are often turbulent (Balachandar & Eaton 2010). Given the complexity of the physical phenomena involved in such flows, they remain relatively poorly

† Email address for correspondence: chibbaro@ida.upmc.fr

https://doi.org/10.1017/jfm.2018.895 Published online by Cambridge University Press

understood and, notably, the formulation of physically sound reduced models is mandatory for practical purposes. To guide this development it is very useful to disentangle the different physical mechanisms at play, and in particular to understand how to cope with the effect of increasing the particle mass loading and the consequent growing importance of collisions and two-way coupling. Indeed, the back reaction exerted by the particles on the fluid gives rise to an extra complexity in modelling (Elghobashi 1994). The understanding of the mechanisms at play, even at a purely qualitative level, is an important subject of research for developing efficient models of relevance to applications (Post & Abraham 2002; Jenny, Roekaerts & Beishuizen 2012; Gualtieri, Battista & Casciola 2017). Unfortunately, it is hard to find clear-cut frontiers between the different regimes (Elghobashi & Truesdell 1992), and thus some heuristic considerations are always needed.

Generally speaking, two classes of probability-density-function (pdf) modelling approaches can be chosen for turbulent flows, namely, Eulerian and Lagrangian (Pope 2000). When the flow is dilute or moderately dense, the Lagrangian pdf approach is mature (Minier, Chibbaro & Pope 2014) and has the desirable features detailed below (Peirano *et al.* 2006). On the other hand, when the volume occupied by the particles is relatively large, collisions are completely dominant, the matter becomes granular, turbulence is absent (or has no effect on the particles) and a hydrodynamic approach is often natural (Puglisi 2014). We consider in this work the intermediate regime of moderately dense turbulent flows, which is less clear.

From a historical perspective, turbulence models for dense flows have been developed in an Eulerian pdf framework on a purely heuristic grounds in analogy with single-phase models (Elghobashi & Abou-Arab 1983; Viollet & Simonin 1994). Only recently, it has been shown that most of those models suffer from some drawbacks and a more rigorous approach has been followed to formulate a complete Reynolds-stress model (Fox 2014). From a modelling point of view, the key, but often overlooked, point for the modelling of turbulent dense flows seems to be the separation between the spatially correlated part, contributing to the turbulent kinetic energy, and the uncorrelated part, responsible for the granular temperature (Dasgupta, Jackson & Sundaresan 1994; Février, Simonin & Squires 2005). This decomposition is motivated by several works in the literature (Capecelatro, Desjardins & Fox 2015, 2016*b*) which pointed out that it leads to a clear distinction between the particle turbulent kinetic energy, related to the spatially correlated part, and the granular temperature due to the uncorrelated part. These two quantities are driven by different mechanisms and therefore need to be modelled separately in moderately dense flows (Capecelatro *et al.* 2015). In particular, owing to the fact that particle–particle collisions are driven by the spatially uncorrelated velocity component, this decomposition is thought to be crucial for collisional flows. Based upon this decomposition, we have developed in the present work a Lagrangian pdf approach, which leads to a stochastic model for the particle phase, that has to be coupled with a consistent Reynolds-stress model for the fluid.

There were several motivations for choosing a Lagrangian pdf approach: (i) it is more intuitive for particle-laden flows and therefore relevant; (ii) some specific issues are particularly arduous to tackle in the Eulerian pdf approach, requiring the Lagrangian one, namely, local but nonlinear phenomena like polydispersity and chemical reactions (Pope 2000; Fox 2003); (iii) the Lagrangian pdf approach provides more detailed information, in particular the velocity of the fluid seen by particles is available whereas it is not in Eulerian pdf models; moreover, it is possible to capture the crossing-trajectory effect due to the mean drift of particles due to the

https://doi.org/10.1017/jfm.2018.895 Published online by Cambridge University Press

spatial variation of fluid velocity (Minier & Peirano 2001); (iv) the possibility of testing different models will provide insights into the role of each term, notably the granular energy, in the development of the particle and fluid turbulence; (v) it is quite difficult to propose sound and realisable Eulerian moment equations for the particle phase, wherein many terms appear unclosed. The development of the Lagrangian pdf approach also helps to derive consistent Eulerian pdf models, which cannot be derived in other ways.

More specifically, in this work, we test two Lagrangian pdf models describing the particle phase, coupled with Reynolds-averaged Eulerian equations for the fluid phase. The first model is based on the velocity partitioning between correlated and uncorrelated components. The second one is a simplified version, where only the total particle velocity, derived as the sum of the two components, is resolved, leading to the lack of distinction between the particle turbulent kinetic energy and the granular temperature. We focus here on statistically homogeneous turbulence. In particular, the goal of the paper is to understand if the pdf models are able to deal with the momentum and energy exchange between phases, and the particle concentration fluctuations. These ingredients are essential in all moderately dense particle-laden flows, and therefore it is important to use the homogeneous cases in order to isolate their modelling from other complex features present in inhomogeneous configurations (e.g. spatial fluxes). In particular, we are interested in cluster-induced turbulence (CIT), which occurs in fluid–particle flows when (i) the mean mass loading φ, defined by the ratio of the specific masses of the particle and fluid phases, is of order one or larger; and (ii) the difference between the mean phase velocities is non-zero. Interestingly, in statistically stationary flows, fluctuations in particle concentration can generate and sustain fluid-phase turbulence, which we refer to as fully developed CIT. Given that the density ratio ρ_p/ρ_f is very large in gas–particle flows, CIT is ubiquitous in practical engineering and environmental flows when body forces or inlet conditions generate a mean velocity difference, such as the gravity-driven flows studied herein. Some fundamental properties of such flows have been recently studied via Eulerian–Lagrangian numerical simulations (Capecelatro, Desjardins & Fox 2014; Capecelatro *et al.* 2015), which will be used for comparison. Notably, the use of models can be relevant to emphasise the mechanisms underlying the volume-fraction fluctuations.

From a physical point of view, we want to assess the pdf models with respect to their ability to reproduce the statistical features of both the particle and fluid phases at high mass loading. It is well known that turbulent particle-laden flows in the dilute limit, where the fluid-phase turbulence interacts with inertial particles without significant feedback from the particles, display a preferential concentration of particles in certain regions (Balkovsky, Falkovich & Fouxon 2001; Balachandar & Eaton 2010). In particular, it is well established that dilute suspensions of heavy particles in isotropic turbulence will preferentially concentrate in regions of high strain rate and low vorticity (Eaton & Fessler 1994). When two-way coupling between the phases is non-negligible, additional effects may be responsible for enhancing the settling rate and spatial segregation of the particles. Among the possible effects, it is worth mentioning the enhancement of particle settling velocity with increasing volume fraction (Bosse, Kleiser & Meiburg 2006), and the creation of strong anisotropy due to the crossing-trajectory effect (Ferrante & Elghobashi 2003) causing also a drag reduction. However, even more impressive is the situation at higher mass loading, where the fluctuating segregation of particles, together with collisions, have been found to create large clusters that induce turbulence in a fluid otherwise at rest

https://doi.org/10.1017/jfm.2018.895 Published online by Cambridge University Press

(Glasser, Sundaresan & Kevrekidis 1998; Capecelatro *et al.* 2015), giving rise to CIT. Notably, in gravity-driven CIT, particles accumulate in regions of low vorticity, as is seen in classical preferential concentration of low-mass-loading suspensions. However, in CIT the vorticity is generated in shear layers between clusters, unlike in classical preferential concentration, where vorticity would exist even in the absence of the disperse phase.

The goal of the present work is precisely to understand whether the proposed pdf models are capable of reproducing quantitatively the phenomena observed in homogeneous particle-laden flows, and also to determine which elements are necessary to trigger the instability leading to CIT.

The paper is organised as follows. In § 2 we derive the exact Lagrangian pdf equations, which are the starting point to build the pdf model. In § 3 the Lagrangian pdf model for the particle phase is presented, followed in § 4 by the one for the fluid velocity seen by particles, and in § 5 the Eulerian Reynolds-averaged (RA) model for the fluid phase. Then, in § 6 RA equations corresponding to the Lagrangian pdf model and in § 7 the complete set of fluid- and particle-phase RA equations are specified for the statistically homogeneous case. In § 8, the models are applied to increasingly more complex particle-laden flows and the results compared to data from the literature, and finally in § 9, conclusions are drawn concerning the relative merits of the proposed pdf models, along with a discussion of future challenges to be faced with applying them to spatially inhomogeneous flows.

2. Rationale for the model construction

When dealing with fluid–particle flows, several levels of description are possible, depending on the amount of information we retain and on the accuracy we are willing to accept. A direct-numerical simulation (DNS) of the Navier–Stokes (NS) equations where the fluid phase is completely resolved around particles, along with the application of no-slip boundary conditions on the particle surface, is what we refer to as the microscopic description (Ten Cate *et al.* 2004; Chouippe & Uhlmann 2015; Picano, Breugem & Brandt 2015; Tanaka 2017). It implies a large amount of information to be handled, since we need a sufficient number of points per particle diameter to describe accurately particle geometry and fluid–particle interactions. Therefore the number of resolved particles is generally limited because of the high computational demand, and this level of description is often unnecessary since particles are small enough to justify a point-wise approximation (Gatignol 1983; Maxey & Riley 1983), even though finite-size effects are important for small systems (Pedley & Kessler 1992), and larger particles (Picano *et al.* 2013; Mehrabadi *et al.* 2018).

Adopting a Lagrangian point of view, small particles with a high particle–fluid density ratio, $\rho_p/\rho_f \gg 1$, can be treated as point particles, where the equation of motion for a particle (k) reduces to

$$\frac{\mathrm{d}\boldsymbol{V}_p^{(k)}}{\mathrm{d}t} = \frac{\boldsymbol{U}_f(\boldsymbol{x}_p) - \boldsymbol{V}_p^{(k)}}{\tau_p} + \boldsymbol{g} + \boldsymbol{A}_c^{(k)}, \tag{2.1}$$

where $\boldsymbol{U}_f(\boldsymbol{x}_p)$ is the fluid velocity at the particle position, $\boldsymbol{g}$ is gravitational acceleration, $\boldsymbol{A}_c$ is the acceleration term due to collisions and τ_p is the particle relaxation time

$$\tau_p = \frac{\rho_p d_p^2}{18\rho_f \nu_f}. \tag{2.2}$$

https://doi.org/10.1017/jfm.2018.895 Published online by Cambridge University Press

Instead of building a pdf model directly on (2.1), we propose to do an intermediate step where we apply a Lagrangian coarse-graining operator, $f^L(\boldsymbol{x}^{(k)}(t), \boldsymbol{V}_p, t)$, to (2.1). This function is the Lagrangian pdf counterpart of the kinetic approach developed for rapid granular flows animated by elastic or inelastic collisions (Jenkins & Savage 1983; Brey *et al.* 1998; Brilliantov & Pöschel 2010), and used in the Eulerian pdf description of turbulent flows (Capecelatro *et al.* 2015). Therefore, this procedure allows us to find a Lagrangian pdf level of description. In particular, this operator is a local average and yields a decomposition of the particle velocity into a spatially correlated component and an uncorrelated one, as initially introduced by Février *et al.* (2005) in the dilute case. Moreover the coarse-graining operator has the following properties: (i) the residual part has zero mean; (ii) the residual part is uncorrelated with the filtered part. With this definition, we have that the hydrodynamic or correlated component is

$$\widetilde{\boldsymbol{V}}_p(\boldsymbol{x}^{(k)}(t), t) = \int \boldsymbol{V}_p f^L(\boldsymbol{x}^{(k)}(t), \boldsymbol{V}_p, t)\, \mathrm{d}\boldsymbol{V}_p, \tag{2.3}$$

and the complete velocity is given by

$$\boldsymbol{V}_p^{(k)} = \widetilde{\boldsymbol{V}}_p(\boldsymbol{x}^{(k)}(t), t) + \boldsymbol{\delta V}_p^{(k)}, \tag{2.4}$$

where we have indicated the coarse-grained quantities with the tilde symbol $\widetilde{\ }$. It is interesting to remark that this coarse-graining shares some similarity with a recent Lagrangian pdf large-eddy simulation filtering formalism applied to particle-laden flows (Innocenti, Marchioli & Chibbaro 2016).

We can now apply the coarse-graining operator to (2.1), neglecting for the moment the effect of collisions:

$$\widetilde{\frac{\mathrm{d}V_{p,i}}{\mathrm{d}t}} = \frac{\partial \widetilde{V}_{p,i}}{\partial t} + \widetilde{V}_{p,j}\frac{\partial \widetilde{V}_{p,i}}{\partial x_j} + \frac{\partial \widetilde{\delta V_{p,i}\delta V_{p,j}}}{\partial x_j} = \frac{\widetilde{U}_{f,i} - \widetilde{V}_{p,i}}{\tau_p} + g_i. \tag{2.5}$$

The Lagrangian transport equation of $\widetilde{V}_{p,i}$ can therefore be expressed as

$$\begin{aligned}\frac{\mathrm{d}\widetilde{V}_{p,i}}{\mathrm{d}t} &= \frac{\partial \widetilde{V}_{p,i}}{\partial t} + V_{p,j}\frac{\partial \widetilde{V}_{p,i}}{\partial x_j} \\ &= \frac{\partial \widetilde{V}_{p,i}}{\partial t} + \widetilde{V}_{p,j}\frac{\partial \widetilde{V}_{p,i}}{\partial x_j} + \delta V_{p,j}\frac{\partial \widetilde{V}_{p,i}}{\partial x_j} \\ &= \frac{\widetilde{U}_{f,i} - \widetilde{V}_{p,i}}{\tau_p} + g_i - \frac{\partial \widetilde{\delta V_{p,i}\delta V_{p,j}}}{\partial x_j} + \delta V_{p,j}\frac{\partial \widetilde{V}_{p,i}}{\partial x_j}.\end{aligned} \tag{2.6}$$

On the other hand, it is also possible to explicitly express the residual part, since its material derivative is given by

$$\begin{aligned}\frac{\mathrm{d}\delta V_{p,i}}{\mathrm{d}t} &= \frac{\mathrm{d}(V_{p,i} - \widetilde{V}_{p,i})}{\mathrm{d}t} \\ &= \frac{\widetilde{U}_{f,i} - V_{p,i}}{\tau_p} + g_i - \frac{\widetilde{U}_{f,i} - \widetilde{V}_{p,i}}{\tau_p} - g_i + \frac{\partial \widetilde{\delta V_{p,i}\delta V_{p,j}}}{\partial x_j} - \delta V_{p,j}\frac{\partial \widetilde{V}_{p,i}}{\partial x_j} \\ &= -\frac{\delta V_{p,i}}{\tau_p} + \frac{\partial \widetilde{\delta V_{p,i}\delta V_{p,j}}}{\partial x_j} - \delta V_{p,j}\frac{\partial \widetilde{V}_{p,i}}{\partial x_j}.\end{aligned} \tag{2.7}$$

https://doi.org/10.1017/jfm.2018.895 Published online by Cambridge University Press

Multiplying (2.7) by $\delta V_{p,j}$ and summing with its transpose term, the Lagrangian transport equation for the uncorrelated energy tensor, i.e. the particle-phase pressure tensor, can be obtained:

$$d(\delta V_{p,i}\delta V_{p,j}) = -2\frac{\delta V_{p,i}\delta V_{p,j}}{\tau_p}\,\mathrm{d}t - \delta V_{p,i}\delta V_{p,k}\frac{\partial \widetilde{V}_{p,j}}{\partial x_k}\,\mathrm{d}t - \delta V_{p,j}\delta V_{p,k}\frac{\partial \widetilde{V}_{p,i}}{\partial x_k}\,\mathrm{d}t + \delta V_{p,i}\frac{\partial \widetilde{\delta V_{p,j}\delta V_{p,k}}}{\partial x_k}\,\mathrm{d}t + \delta V_{p,j}\frac{\partial \widetilde{\delta V_{p,i}\delta V_{p,k}}}{\partial x_k}\,\mathrm{d}t. \tag{2.8}$$

Following this decomposition, we can thus define two different Lagrangian stochastic processes, one for the coarse-grained particle velocity and one for the residual component:

$$\left.\begin{aligned} \mathrm{d}\widetilde{V}_{p,i} &= \frac{\widetilde{U}_{f,i} - \widetilde{V}_{p,i}}{\tau_p}\,\mathrm{d}t + g_i\,\mathrm{d}t - \frac{\partial \widetilde{\delta V_{p,i}\delta V_{p,k}}}{\partial x_k}\,\mathrm{d}t + \delta V_{p,k}\frac{\partial \widetilde{V}_{p,i}}{\partial x_k}\,\mathrm{d}t, \\ \mathrm{d}\delta V_{p,i} &= -\frac{\delta V_{p,i}}{\tau_p}\,\mathrm{d}t + \frac{\partial \widetilde{\delta V_{p,i}\delta V_{p,k}}}{\partial x_k}\,\mathrm{d}t - \delta V_{p,k}\frac{\partial \widetilde{V}_{p,i}}{\partial x_k}\,\mathrm{d}t. \end{aligned}\right\} \tag{2.9}$$

These equations are the Lagrangian pdf counterpart of the Eulerian equations of Jenkins & Savage (1983) and Capecelatro *et al.* (2015) and we will refer to them as Lagrangian pdf equations.

It is important to underline that this picture is valid for a given fluid realisation. For laminar flows, which are not sensitive to initial and boundary conditions, the flow is always the same, independent of the realisation, given the geometry and the initial state. For turbulent flows, the situation is more complicated and, because of the inevitable presence of small perturbations, the instantaneous field changes at each realisation. Therefore if one performs averages of the relevant observables over different realisations, the statistical quantities obtained are the Reynolds-averaged (RA) ones. In particular, the RA transport equations obtained from (2.9) (reported in appendix A), are not closed and cannot be used without a modelling step. Instead of modelling directly the RA equations, as done for instance by Capecelatro *et al.* (2016*b*), we model here the Lagrangian pdf equations through a stochastic approach in order to retrieve the correct terms in an average sense.

3. Lagrangian pdf model for the particle phase

To clearly explain the derivation of the pdf model, we need to introduce some concepts related to the averaging procedure. Keeping in mind the definition of a phase average (PA) (Capecelatro *et al.* 2015), where a quantity is weighted with the volume fraction when averaging, we recall that the RA of a Lagrangian quantity is also a PA, since we are implicitly weighting with the phase volume fraction. In particular, if we indicate the average with brackets $\langle\cdot\rangle$, we will have for the fluid phase $\langle(\cdot)\rangle_f = \langle\alpha_f(\cdot)\rangle/\langle\alpha_f\rangle$ and for the particle phase $\langle(\cdot)\rangle_p = \langle\alpha_p(\cdot)\rangle/\langle\alpha_p\rangle$, where $\langle\alpha_p\rangle$ and $\langle\alpha_f\rangle = 1 - \langle\alpha_p\rangle$ are respectively the particle-phase and the fluid-phase volume fractions. To simplify the notation we will drop the subscript indicating the phase, except when doing cross-averages, as for instance a fluid quantity weighted with the particle volume fraction.

From the definition of the coarse-graining operator given in § 2, we have that

$$\langle\widetilde{\boldsymbol{V}}_p\rangle = \langle\boldsymbol{V}_p\rangle, \quad \langle\delta\boldsymbol{V}_p\rangle = 0. \tag{3.1a,b}$$

https://doi.org/10.1017/jfm.2018.895 Published online by Cambridge University Press

The total particle-phase fluctuating energy is defined by

$$\kappa_p = \tfrac{1}{2}\langle \boldsymbol{v}_p \cdot \boldsymbol{v}_p \rangle, \tag{3.2}$$

where $\boldsymbol{v}_p = \boldsymbol{V}_p - \langle \boldsymbol{V}_p \rangle$ is the total fluctuation in the particle velocity, which can also be expressed as the sum of two contributions: the fluctuation of the coarse-grained, correlated part, $\widetilde{\boldsymbol{v}}_p = \widetilde{\boldsymbol{V}}_p - \langle \widetilde{\boldsymbol{V}}_p \rangle$, and the uncorrelated part, $\delta \boldsymbol{V}_p$. By means of this decomposition, the total particle-phase fluctuating energy can, in turn, be split in two contributions, the turbulent particle-phase kinetic energy and the granular temperature:

$$\kappa_p = k_p + \tfrac{3}{2}\langle \Theta_p \rangle, \tag{3.3}$$

where

$$k_p = \tfrac{1}{2}\langle \widetilde{\boldsymbol{v}}_p \cdot \widetilde{\boldsymbol{v}}_p \rangle \quad \langle \Theta \rangle_p = \tfrac{1}{3}\langle \widetilde{\delta \boldsymbol{V}_p \cdot \delta \boldsymbol{V}_p} \rangle. \tag{3.4a,b}$$

The granular temperature can equally be found from the trace of the particle-phase pressure tensor

$$\langle \boldsymbol{P} \rangle = \langle \widetilde{\delta \boldsymbol{V}_p \otimes \delta \boldsymbol{V}_p} \rangle. \tag{3.5}$$

The distinction between k_p and $\langle \Theta_p \rangle$, as already said, is crucial in turbulence modelling of multiphase flows because, for example, they have different boundary conditions and the particle–particle collision frequency depends on Θ_p (Capecelatro *et al.* 2016*b*).

3.1. *Modelled equations*

To distinguish modelled terms from exact ones, we will call $\boldsymbol{U}_p$ the model for $\widetilde{\boldsymbol{V}}_p$, and $\delta \boldsymbol{v}_p$ the model for $\delta \boldsymbol{V}_p$. It is worth recalling that $\boldsymbol{U}_p$ and $\delta \boldsymbol{v}_p$ are two stochastic processes modelling the particle total velocity, and therefore they are both advected by it, i.e. by $\boldsymbol{V}_p = \boldsymbol{U}_p + \delta \boldsymbol{v}_p$.

Keeping in mind (2.9), the principle that drives the modelling is to retain the closed terms (drag force), which can be expressed exactly, while the transport terms, which involve spatial gradients (last two terms in (2.9)), are split into a mean part and a fluctuation. The mean part, being available from Lagrangian averages, is plugged into the model, while fluctuations are modelled through white noises and drift terms. Those terms have been constructed in order to give the correct RA equations when compared to the exact ones in appendix A. We recall that RA quantities can be found as statistical moments of the underlying pdf.

The proposed stochastic model for the particle phase reads

$$\mathrm{d}x_{p,i} = V_{p,i}\,\mathrm{d}t = (U_{p,i} + \delta v_{p,i})\,\mathrm{d}t, \tag{3.6}$$

$$\begin{aligned} \mathrm{d}U_{p,i} \;=\; & \frac{U_{s,i} - U_{p,i}}{\tau_p}\,\mathrm{d}t + g_i\,\mathrm{d}t - \frac{1}{\langle \alpha_p \rangle \rho_p}\frac{\partial \langle \alpha_p \rangle \rho_p \langle P_{ij} \rangle}{\partial x_j} + \delta v_{p,j}\frac{\partial \langle U_{p,i} \rangle}{\partial x_j}\,\mathrm{d}t \\ & - \frac{1}{T_{Lp}}(U_{p,i} - \langle U_{p,i} \rangle)\,\mathrm{d}t + \sqrt{C_p \varepsilon_p}\,\mathrm{d}W_{p,i}, \end{aligned} \tag{3.7}$$

$$\begin{aligned} \mathrm{d}\delta v_{p,i} \;=\; & -\frac{\delta v_{p,i}}{\tau_p}\,\mathrm{d}t + \frac{1}{\langle \alpha_p \rangle \rho_p}\frac{\partial \langle \alpha_p \rangle \rho_p \langle P_{ij} \rangle}{\partial x_j} - \delta v_{p,j}\frac{\partial \langle U_{p,i} \rangle}{\partial x_j}\,\mathrm{d}t + B_{\delta,ij}\,\mathrm{d}W_{\delta,j} \\ & - \frac{(1+e)(3-e)}{4\tau_c}\delta v_{p,i}\,\mathrm{d}t + \sqrt{\frac{1}{2\tau_c}(1+e)^2 \langle \Theta_p \rangle}\,\mathrm{d}W_{c,i}. \end{aligned} \tag{3.8}$$

https://doi.org/10.1017/jfm.2018.895 Published online by Cambridge University Press

The first term on the right-hand side of (3.7) is the drag force related to the correlated part of the particle velocity, in which $\boldsymbol{U}_s$ stands for the model for $\widetilde{\boldsymbol{U}}_f$, the fluid velocity seen by the particle (whose expression will be given in the following) and τ_p the particle relaxation time. The second term is the effect of gravity, $\boldsymbol{g}$, while the third is a pressure term, in which ρ_p is the particle density, α_p the particle-phase volume fraction and $\langle P_{ij}\rangle = \langle \delta v_{p,i} \delta v_{p,j}\rangle$ is the particle-phase pressure tensor. The fourth and fifth terms are production and relaxation, respectively, in which T_{Lp} is the particle Lagrangian time scale defined by

$$T_{Lp} = \left(\frac{1}{2} + \frac{3}{4}C_{0p} + \frac{f_s}{2}\right)^{-1} \frac{k_p}{\varepsilon_p}, \tag{3.9}$$

where $k_p = (1/2)\langle \boldsymbol{u}_p \cdot \boldsymbol{u}_p\rangle$ is the particle-phase turbulent kinetic energy with $\boldsymbol{u}_p = \boldsymbol{U}_p - \langle \boldsymbol{U}_p\rangle$, ε_p represents the particle-phase dissipation, to be specified shortly, and C_{0p} is a free parameter equivalent to C_0 for the fluid Lagrangian time (Pope 2000). Finally, the last contribution is a diffusion term, in which C_p is a model constant to be *a priori* assigned and $\mathrm{d}W_{p,i}$ is a Wiener stochastic process (Gardiner 1990). The constant C_p in the diffusion coefficient of (3.7) is related to the Lagrangian time scale to obtain a redistribution tensor and a dissipation tensor, by the relation

$$C_p = C_{0p} + \tfrac{2}{3} f_s. \tag{3.10}$$

The parameter f_s is introduced to account for anisotropy in the particle-phase dissipation tensor (Capecelatro *et al.* 2016*b*), which is needed to predict the anisotropy of the particle-phase pressure tensor $\langle \boldsymbol{P}\rangle$. The last two terms in (3.7) in particular, are those used to model unclosed fluctuations in (2.9) and they give at the RA level a redistribution and a dissipation term (ε_p) in the equation of the particle Reynolds stresses.

The first four terms on the right-hand side of (3.8) are analogous to the ones in (3.7). However, in order to obtain the correct averaged equations, we have had to break the original symmetry of the two parts. In particular, while the averaged terms are the same for the correlated and uncorrelated parts, the fluctuating ones cannot be. In the model for the fluctuations, $\mathrm{d}W_\delta$ is a Wiener process and B_δ is a diffusion matrix, whose expression is given in the following. The last two terms take into account collisions; e is a restitution coefficient, to be *a priori* specified, $\mathrm{d}W_{c,i}$ is another Wiener process uncorrelated with $\mathrm{d}W_{\delta,i}$, since they represent different physics, and $\langle \Theta_p\rangle$ is the granular temperature, defined as $\langle \Theta_p\rangle = (1/3)\langle \delta \boldsymbol{v}_p \cdot \delta \boldsymbol{v}_p\rangle$. Finally, τ_c is a characteristic time for collisions, having the following expression:

$$\tau_c = \frac{\sqrt{\pi}\, d_p}{6 C_c \langle \alpha_p\rangle \langle \Theta_p\rangle^{1/2}}, \tag{3.11}$$

d_p being the particle diameter and C_c a model parameter (Capecelatro *et al.* 2016*b*). This Lagrangian model for collisions gives, at the RA level, the same model as in Capecelatro *et al.* (2016*b*). This collision model is applicable to rapid granular flows that can be modelled by the Boltzmann equation with inelastic hard-sphere collisions, i.e. the collisional and frictional contributions are not accounted for in the particle-phase pressure tensor.

https://doi.org/10.1017/jfm.2018.895 Published online by Cambridge University Press

When the correlation $\langle \delta v_{p,i} \delta v_{p,j} \rangle$ is evaluated, the diffusion matrix $\boldsymbol{B}_\delta$ must give the particle-phase Reynolds stress multiplied by the proper coefficient added to a diagonal isotropic part. Using the Cholesky decomposition (see appendix B) we obtain

$$\left.\begin{aligned} B_{\delta,11} &= \left(f_s \frac{\varepsilon_p}{k_p} \langle u_{p,1} u_{p,1} \rangle + (1 - f_s) \frac{2}{3} \varepsilon_p \right)^{1/2}, \\ B_{\delta,i1} &= \frac{1}{B_{\delta,11}} \left(f_s \frac{\varepsilon_p}{k_p} \langle u_{p,i} u_{p,1} \rangle \right), \quad 1 < i \leqslant 3, \\ B_{\delta,ii} &= \left(f_s \frac{\varepsilon_p}{k_p} \langle u_{p,i} u_{p,i} \rangle + (1 - f_s) \frac{2}{3} \varepsilon_p - \sum_{j=1}^{i-1} B_{\delta,ij}^2 \right)^{1/2}, \quad 1 < i \leqslant 3, \\ B_{\delta,ij} &= \frac{1}{B_{\delta,jj}} \left(f_s \frac{\varepsilon_p}{k_p} \langle u_{p,i} u_{p,j} \rangle - \sum_{k=1}^{j-1} B_{\delta,ik} B_{\delta,jk} \right), \quad 1 < j < i \leqslant 3, \\ B_{\delta,ij} &= 0, \quad i < j \leqslant 3, \end{aligned}\right\} \tag{3.12}$$

where repeated indices do not imply summation.

As in Lagrangian pdf methods for single-phase flows (Pope 2000), it should be borne in mind that such a model is intended to represent the pdf, or the statistical moments, associated with the particle phase, and not the instantaneous particle dynamics, which is 'fictitious'.

4. Lagrangian pdf model for the fluid seen by particles

The equation for the particle velocity (3.7) contains the velocity of the fluid at the position of the particle, or the fluid seen by particles. Since in Reynolds averaged Navier–Stokes (RANS) simulations we have no access to this quantity, nor to its average, a model for it has to be specified. Furthermore, given that we are considering flow with two-way coupling, this effect has to be included also in the fluid-phase equation. We develop in this section a new stochastic model for $\boldsymbol{U}_s$, which will be a Langevin equation of the type

$$\mathrm{d}U_{s,i} = [A_{s,i} + A_{p \to s,i}]\, \mathrm{d}t + B_{s,ij}\, \mathrm{d}W_{s,j}, \tag{4.1}$$

where $A_{p \to s,i}$ represents explicitly the effect of the particles on the fluid, and $\mathrm{d}W_{s,j}$ is a different Wiener process from those present in (3.7) and (3.8). The drift term, $\boldsymbol{A}_s$, is modelled following the path pointed out for dilute flows (Minier & Peirano 2001; Minier, Peirano & Chibbaro 2004; Peirano *et al.* 2006):

$$A_{s,i} = -\frac{\langle \alpha_f \rangle}{\rho_f} \frac{\partial \langle p_f \rangle}{\partial x_i} + (\langle U_{p,j} \rangle - \langle U_{f,j} \rangle) \frac{\partial \langle U_{f,i} \rangle}{\partial x_j} + G_{ij} \left(U_{s,j} - \langle U_{f,j} \rangle \right) + g_i. \tag{4.2}$$

The first term on the right-hand side is the pressure-gradient term, where ρ_f is the fluid density and p_f the fluid pressure, which models the fluid pressure gradient seen by particles. In general, the subscript f denotes a flow variable in the fluid phase. This pressure term has been weighted by the local averaged fluid volume fraction in order to model the possible presence of a drift velocity even in homogeneous flows. The second term models the crossing-trajectory effect (CTE), while the third term is a relaxation term, where

$$G_{ij} = -\frac{1}{T^*_{L,i}} \delta_{ij} + G^a_{ij} \tag{4.3}$$

https://doi.org/10.1017/jfm.2018.895 Published online by Cambridge University Press

is the matrix defining the corresponding Reynolds-stress model. The first part is the simplified Langevin model (SLM) adapted to the inertial particles, while $\boldsymbol{G}^a$ is a traceless matrix to be added to generalise the model. For instance, the Launder–Reece–Rodi model (Launder, Reece & Rodi 1975) (LRR-IP) model reads

$$G^a_{ij} = C_{2f}\frac{\partial \langle U_{f,i}\rangle}{\partial x_j} \tag{4.4}$$

and C_{2f} is the isotropisation-of-production (IP) constant, usually taken $C_{2f} = (3/5)$ consistent with rapid-distortion theory.

$T^*_{L,i}$ is a modified time scale that take into account particle inertia according to Csanady's analysis:

$$T^*_{L,i} = \frac{T_{Lf}}{\sqrt{1 + \zeta_i \beta^2 \dfrac{3|\langle \boldsymbol{U}_r\rangle|^2}{2k_f}}}, \tag{4.5}$$

where

$$T_{Lf} = \frac{1}{\left(\frac{1}{2} + \frac{3}{4}C_{0f}\right)}\frac{k_f}{\varepsilon_f} \tag{4.6}$$

is the Lagrangian time scale, C_{0f} being linked to the Rotta constant by the relation

$$C_{0f} = \tfrac{2}{3}(C_R - 1), \tag{4.7}$$

and the relative velocity is defined by

$$\boldsymbol{U}_r = \boldsymbol{U}_p - \boldsymbol{U}_s. \tag{4.8}$$

Moreover, $\zeta_1 = 1$ in the mean drift direction and $\zeta_{2,3} = 4$ in the cross-directions, $\beta = T_{Lf}/T_{Ef}$ is the ratio of the Lagrangian and Eulerian time scales (Wang & Stock 1993).

The modelling of the two-way coupling term instead is as follows. The exact expression for the two-way coupling term, $\boldsymbol{A}_{p\to s}$, which is induced by the presence of the discrete particles, is not *a priori* known. The underlying force corresponds to the exchange of momentum between the fluid and particles, but should not be confused with the total force acting on particles since the latter includes external forces such as gravity. The effect of particles on fluid properties is expressed directly in the model for $\boldsymbol{U}_s$ through a simple stochastic equation. The force exerted by one particle on the fluid corresponds to the drag force written here as

$$\boldsymbol{F}_{p\to f} = -m_p\frac{\boldsymbol{U}_s - \boldsymbol{U}_p}{\tau_p}, \tag{4.9}$$

where m_p is the mass of a particle. The total force acting on the fluid element surrounding a discrete particle is then obtained as the sum of all elementary forces, $\boldsymbol{F}_{p\to f}$, and the resulting acceleration is modelled here as (Peirano & Minier 2002)

$$A_{p\to s,i} = -\varphi\frac{U_{s,i} - U_{p,i}}{\tau_p}, \tag{4.10}$$

where φ is the mean mass loading, $\varphi = (\langle\alpha_p\rangle\rho_p/\langle\alpha_f\rangle\rho_f)$.

https://doi.org/10.1017/jfm.2018.895 Published online by Cambridge University Press

4.1. *Closure of the diffusion coefficient*

The drift terms are given by (4.2) and (4.10), but the diffusion coefficient needs to be specified in order to obtain a complete closure. Analogously to dilute flows, we look for a diffusion matrix in a diagonal, but anisotropic form. To close this term, we consider the decay of the turbulent kinetic energy in the homogeneous case, in absence of mean shear, and we make the following assumption:

$$\frac{\mathrm{d}k_f}{\mathrm{d}t} \simeq \frac{\mathrm{d}k_{f@p}}{\mathrm{d}t}, \tag{4.11}$$

where $k_f = (1/2)\langle \boldsymbol{u}_f \cdot \boldsymbol{u}_f \rangle$ is the turbulent kinetic energy of the fluid phase, with $\boldsymbol{u}_f = \boldsymbol{U}_f - \langle \boldsymbol{U}_f \rangle$ the fluid fluctuation, and $k_{f@p} = (1/2)\langle \boldsymbol{u}_f \cdot \boldsymbol{u}_f \rangle_p$ is the turbulent kinetic energy of the fluid phase seen by the particles. It is worth recalling that fluid-phase RA terms such as k_f and $\langle U_{f,i} \rangle$ are known from the RA transport equation, which will be presented in § 5. A possible alternative could be to impose an analogous relation, but for all the Reynolds-stress components, which would lead to a much more complex model.

Recalling the phase averaging introduced in § 3, we can obtain the following equality for the fluid velocity fluctuations:

$$\langle \boldsymbol{u}_f \rangle_p = \langle \boldsymbol{U}_f - \langle \boldsymbol{U}_f \rangle_f \rangle_p = \langle \boldsymbol{U}_s \rangle - \langle \boldsymbol{U}_f \rangle. \tag{4.12}$$

Thus, (4.11) can be rewritten as

$$\frac{\mathrm{d}k_f}{\mathrm{d}t} = \frac{1}{2}\frac{\mathrm{d}}{\mathrm{d}t}\sum_{i=1}^{3}[\langle U_{s,i}^2 \rangle + \langle U_{f,i} \rangle^2 - 2\langle U_{s,i} \rangle \langle U_{f,i} \rangle], \tag{4.13}$$

where time variations of the fluid velocity and the fluid velocity seen by particles in the homogeneous case are expressed by

$$\frac{\mathrm{d}\langle U_{f,i} \rangle}{\mathrm{d}t} = f_i + g_i + \varphi \frac{\langle U_{p,i} - U_{s,i} \rangle}{\tau_p}, \tag{4.14}$$

$$\mathrm{d}U_{s,i} = \langle \alpha_f \rangle f_i \,\mathrm{d}t - \frac{1}{T_{L,i}^*}(U_{s,i} - \langle U_{f,i} \rangle)\,\mathrm{d}t + g_i \,\mathrm{d}t + \varphi \frac{U_{p,i} - U_{s,i}}{\tau_p}\,\mathrm{d}t + B_{s,ii}\,\mathrm{d}W_{s,i}, \tag{4.15}$$

$$\begin{aligned}\frac{\mathrm{d}\langle U_{s,i}^2 \rangle}{\mathrm{d}t} &= 2\langle \alpha_f \rangle f_i \langle U_{s,i} \rangle - \frac{2}{T_{L,i}^*}\langle U_{s,i}^2 \rangle + \frac{2}{T_{L,i}^*}\langle U_{s,i} \rangle \langle U_{f,i} \rangle + 2g_i \langle U_{s,i} \rangle \\ &\quad + 2\varphi \frac{\langle U_{p,i} U_{s,i} \rangle - \langle U_{s,i}^2 \rangle}{\tau_p} + B_{s,ii}^2,\end{aligned} \tag{4.16}$$

$$\frac{\mathrm{d}\langle U_{f,i} \rangle^2}{\mathrm{d}t} = 2\langle U_{f,i} \rangle \frac{\mathrm{d}\langle U_{f,i} \rangle}{\mathrm{d}t} = 2f_i \langle U_{f,i} \rangle + 2g_i \langle U_{f,i} \rangle + 2\varphi \langle U_{f,i} \rangle \frac{\langle U_{p,i} - U_{s,i} \rangle}{\tau_p}, \tag{4.17}$$

$$\begin{aligned}\frac{\mathrm{d}\langle U_{s,i} \rangle \langle U_{f,i} \rangle}{\mathrm{d}t} &= -\frac{1}{T_{L,i}^*}(\langle U_{f,i} \rangle \langle U_{s,i} \rangle - \langle U_{f,i} \rangle^2) + f_i(\langle \alpha_f \rangle \langle U_{f,i} \rangle + \langle U_{s,i} \rangle) \\ &\quad + g_i(\langle U_{f,i} \rangle + \langle U_{s,i} \rangle) + \varphi \langle U_{f,i} \rangle \frac{\langle U_{p,i} - U_{s,i} \rangle}{\tau_p} + \varphi \langle U_{s,i} \rangle \frac{\langle U_{p,i} - U_{s,i} \rangle}{\tau_p},\end{aligned} \tag{4.18}$$

https://doi.org/10.1017/jfm.2018.895 Published online by Cambridge University Press

with $f_i = -(1/\rho_f)\partial\langle p_f\rangle/\partial x_i$. Now, if we substitute (4.16)–(4.18) into (4.13), the following relation is obtained:

$$\frac{\mathrm{d}k_f}{\mathrm{d}t} = -\varepsilon_f + \sum_{i=1}^{3}\left[\varphi\frac{\langle U_{p,i}U_{s,i}\rangle - \langle U_{s,i}^2\rangle}{\tau_p} - \varphi\langle U_{f,i}\rangle\frac{\langle U_{p,i}-U_{s,i}\rangle}{\tau_p}\right]$$
$$= \sum_{i=1}^{3}\left[-\frac{1}{T_{L,i}^*}\langle(U_{s,i}-\langle U_{f,i}\rangle)^2\rangle - \langle\alpha_p\rangle f_i(\langle U_{s,i}\rangle - \langle U_{f,i}\rangle) + \frac{B_{s,ii}^2}{2} + \varphi\frac{\langle u_{p,i}u_{s,i}\rangle - \langle u_{s,i}^2\rangle}{\tau_p}\right]. \tag{4.19}$$

The terms $(1/T_{L,i}^*)\langle(U_{s,i}-\langle U_{f,i}\rangle)^2\rangle$ and ε_f can be rearranged together, whereas the other terms are redistributed on each corresponding component shown above. The result is

$$B_{s,ii}^2 = 2\varphi\frac{\langle U_{p,i}-U_{s,i}\rangle}{\tau_p}(\langle U_{s,i}\rangle - \langle U_{f,i}\rangle) + 2\langle\alpha_p\rangle f_i(\langle U_{s,i}\rangle - \langle U_{f,i}\rangle)$$
$$+ \varepsilon_f\left[C_0 b_i\frac{\tilde{k}_f}{k_f} + \frac{2}{3}\left(b_i\frac{\tilde{k}_f}{k_f} - 1\right)\right], \tag{4.20}$$

with $b_i = T_L/T_{L,i}^*$ and

$$\tilde{k}_f = \frac{3}{2}\frac{\sum_{i=1}^{3} b_i\langle(U_{s,i}-\langle U_{f,i}\rangle)^2\rangle}{\sum_{i=1}^{3} b_i}. \tag{4.21}$$

Therefore the final form of the Lagrangian pdf equation for the fluid velocity seen by particles, to be coupled with (3.6)–(3.8) for the particle position and velocity, is

$$\mathrm{d}U_{s,i}(t) = -\frac{\langle\alpha_f\rangle}{\rho_f}\frac{\partial\langle p_f\rangle}{\partial x_i}\,\mathrm{d}t + (\langle U_{p,j}\rangle - \langle U_{f,j}\rangle)\frac{\partial\langle U_{f,i}\rangle}{\partial x_j}\,\mathrm{d}t$$
$$+ G_{ij}(U_{s,j} - \langle U_{f,j}\rangle)\,\mathrm{d}t - \varphi\left(\frac{U_{s,i}-U_{p,i}}{\tau_p}\right)\mathrm{d}t + g_i\,\mathrm{d}t$$
$$+ \left[\varepsilon_f\left(C_0 b_i\frac{\tilde{k}_f}{k_f} + \frac{2}{3}\left(b_i\frac{\tilde{k}_f}{k_f} - 1\right)\right) + 2\varphi\frac{\langle U_{p,i}-U_{s,i}\rangle}{\tau_p}(\langle U_{s,i}\rangle - \langle U_{f,i}\rangle)\right.$$
$$\left. - 2\frac{\langle\alpha_p\rangle}{\rho_f}\frac{\partial\langle p_f\rangle}{\partial x_i}(\langle U_{s,i}\rangle - \langle U_{f,i}\rangle)\right]^{1/2}\mathrm{d}W_{s,i}. \tag{4.22}$$

It is worth remarking that in the presence of a mean shear, the anisotropic term G_{ij}^a should also be considered in the derivation of the diffusion coefficient, which will give rise to an additional term in (4.20) in analogy with single-phase flows (Pope 1994):

$$\tfrac{2}{3}C_{2f}\mathcal{P}_{Sfs}, \tag{4.23}$$

where $\mathcal{P}_{Sfs}$ is one half of the trace of the tensor

$$\boldsymbol{\mathcal{P}}_{Sfs} = -(\langle(\boldsymbol{U}_s - \langle\boldsymbol{U}_f\rangle)\otimes(\boldsymbol{U}_s - \langle\boldsymbol{U}_f\rangle)\rangle\cdot\nabla\langle\boldsymbol{U}_f\rangle)^{\dagger}, \tag{4.24}$$

https://doi.org/10.1017/jfm.2018.895 Published online by Cambridge University Press

where the symbol $(\cdot)^{\dagger}$ implies the summation of a second-order tensor with its transpose. The set of equations for the particle and fluid velocities can be recast in vector form as follows:

$$\mathrm{d}\boldsymbol{X} = \boldsymbol{A}\,\mathrm{d}t + [B]\,\mathrm{d}\boldsymbol{W}, \tag{4.25}$$

where $\boldsymbol{A}$ is the drift term, and

$$\boldsymbol{X} = \begin{pmatrix} \boldsymbol{U}_p \\ \delta\boldsymbol{v}_p \\ \boldsymbol{U}_s \end{pmatrix}, \quad [B] = \begin{bmatrix} C[I] & 0 & 0 & 0 \\ 0 & [B_\delta] & K[I] & 0 \\ 0 & 0 & 0 & [B_s] \end{bmatrix}, \quad \mathrm{d}\boldsymbol{W} = \begin{pmatrix} \mathrm{d}\boldsymbol{W}_p \\ \mathrm{d}\boldsymbol{W}_\delta \\ \mathrm{d}\boldsymbol{W}_c \\ \mathrm{d}\boldsymbol{W}_s \end{pmatrix}, \tag{4.26}$$

$C = \sqrt{C_p\varepsilon_p}$ is the diagonal diffusion coefficient in the equation of the correlated velocity and $K = \sqrt{1/(2\tau_c)(1+e^2)\langle\Theta_p\rangle}$ is the diagonal diffusion coefficient for the collisions in the uncorrelated velocity equation.

5. Eulerian pdf model for the fluid phase

The RA fluid-phase equations (A 4)–(A 7) could easily be replaced by a suitable RANS model (k–ε, Reynolds-stress models, see Pope (2000)); however, single-phase turbulence models typically do not take into account two-way coupling between the phases. Thus, both in the momentum and in the Reynolds-stress equations, we need to formulate the terms that mimic this effect. We follow here the approach first proposed by Peirano & Minier (2002). We consider the direct effect of the particles on the fluid through a random acceleration. Since a fluid and a discrete particle will not be present at the same spatial position in the same instant with probability one, we define this random acceleration as

$$\boldsymbol{A}_{pf} \equiv \frac{\rho_p}{\rho_f}\frac{\boldsymbol{U}_p - \boldsymbol{U}_s}{\tau_p}, \tag{5.1}$$

with a probability $\langle\alpha_p\rangle(t, \boldsymbol{x}_f)$, where $\boldsymbol{A}_{pf}$ is a random variable which is formed from the discrete particles at the location $\boldsymbol{x}_p = \boldsymbol{x}$.

In other words, from the stochastic models for the discrete particles, or from the one-point particle pdf value at location $\boldsymbol{x} = \boldsymbol{x}_f$, we form the random variables $\boldsymbol{A}_{pf}$ with the same distribution. This random term mimics the reverse forces due to the discrete particles and is only non-zero where the fluid particle is in the close neighbourhood of a discrete particle. At the location $\boldsymbol{x}$ considered, $\boldsymbol{A}_{pf}$ is defined as a random acceleration term in the equation for $\boldsymbol{U}_f$, correlated with $\boldsymbol{U}_f$, so that we have

$$\langle\boldsymbol{A}_{pf}\rangle = \frac{\rho_p}{\rho_f}\left\langle\frac{\boldsymbol{U}_p - \boldsymbol{U}_s}{\tau_p}\right\rangle = \frac{\rho_p}{\rho_f}\left\langle\frac{\boldsymbol{U}_p - \boldsymbol{U}_f}{\tau_p}\right\rangle_p, \tag{5.2a}$$

$$\langle\boldsymbol{A}_{pf}\otimes\boldsymbol{U}_f\rangle = \frac{\rho_p}{\rho_f}\left\langle\frac{(\boldsymbol{U}_p - \boldsymbol{U}_s)\otimes\boldsymbol{U}_s}{\tau_p}\right\rangle = \frac{\rho_p}{\rho_f}\left\langle\frac{(\boldsymbol{U}_p - \boldsymbol{U}_f)\otimes\boldsymbol{U}_f}{\tau_p}\right\rangle_p. \tag{5.2b}$$

Thus, the resulting RA equations for the fluid phase will be

$$\frac{\partial}{\partial t}(\langle\alpha_f\rangle\rho_f) + \boldsymbol{\nabla}\cdot(\langle\alpha_f\rangle\rho_f\langle\boldsymbol{U}_f\rangle) = 0, \tag{5.3}$$

https://doi.org/10.1017/jfm.2018.895 Published online by Cambridge University Press

$$\frac{\partial \langle\alpha_f\rangle\langle \boldsymbol{U}_f\rangle}{\partial t} + \boldsymbol{\nabla}\cdot\langle\alpha_f\rangle(\langle \boldsymbol{U}_f\rangle \otimes \langle \boldsymbol{U}_f\rangle + \langle \boldsymbol{u}_f \otimes \boldsymbol{u}_f\rangle) = -\frac{\langle\alpha_f\rangle}{\rho_f}\boldsymbol{\nabla}\langle p_f\rangle + \langle\alpha_f\rangle\nu\nabla^2\langle \boldsymbol{U}_f\rangle + \frac{\langle\alpha_p\rangle\rho_p}{\rho_f}\left\langle\frac{\boldsymbol{U}_p - \boldsymbol{U}_s}{\tau_p}\right\rangle + \langle\alpha_f\rangle\boldsymbol{g}. \tag{5.4}$$

The resulting Reynolds-stress transport equation is closed here by the LRR-IP model (Pope 2000), and the two-way coupling term of (5.2*b*):

$$\frac{\partial \langle\alpha_f\rangle\langle \boldsymbol{u}_f \otimes \boldsymbol{u}_f\rangle}{\partial t} + \boldsymbol{\nabla}\cdot\langle\alpha_f\rangle(\langle \boldsymbol{U}_f\rangle \otimes \langle \boldsymbol{u}_f \otimes \boldsymbol{u}_f\rangle) = \boldsymbol{\nabla}\cdot(\langle\alpha_f\rangle\nu\boldsymbol{\nabla}\langle \boldsymbol{u}_f \otimes \boldsymbol{u}_f\rangle) + \boldsymbol{\mathcal{L}} + \langle\alpha_f\rangle\boldsymbol{\mathcal{P}}_f + \langle\alpha_f\rangle\boldsymbol{\mathcal{R}}_f - \frac{2}{3}\langle\alpha_f\rangle\varepsilon_f\boldsymbol{I} + \langle\alpha_p\rangle[\langle\boldsymbol{\Pi}_p \otimes \boldsymbol{U}_f\rangle - \langle \boldsymbol{U}_f\rangle \otimes \langle\boldsymbol{\Pi}_p\rangle]^{\dagger}. \tag{5.5}$$

The turbulent mean-gradient-production term is defined by

$$\boldsymbol{\mathcal{P}}_f = -(\langle \boldsymbol{u}_f \otimes \boldsymbol{u}_f\rangle\cdot\boldsymbol{\nabla}\langle \boldsymbol{U}_f\rangle)^{\dagger} \tag{5.6}$$

and the pressure-redistribution term is modelled by

$$\boldsymbol{\mathcal{R}}_f = -C_{Rf}\frac{\varepsilon_f}{k_f}\left(\langle \boldsymbol{u}_f \otimes \boldsymbol{u}_f\rangle - \frac{2}{3}k_f\boldsymbol{I}\right) - C_{2f}\left(\boldsymbol{\mathcal{P}}_f - \frac{2}{3}\mathcal{P}_f\boldsymbol{I}\right). \tag{5.7}$$

The transport term $\boldsymbol{\mathcal{L}}$ may be modelled with the different standard models present in the literature (Pope 2000). Here we leave it in an unclosed form, since it does not play a role in the homogeneous flows presented hereinafter.

Some remarks are in order concerning the fluid-phase Reynolds-stress model. Following Capecelatro *et al.* (2016*b*), we have chosen the LRR-IP model, which is widely used and gives reasonably good results, but any other realisable Reynolds-stress model could be chosen, if needed. The important point is that it has been demonstrated that a realisable Reynolds-stress model exists for every Lagrangian pdf model for the fluid (Pope 1994). Furthermore, consistency between Eulerian and Lagrangian models of the fluid should be always assured (Muradoglu, Pope & Caughey 2001; Chibbaro & Minier 2011; Minier *et al.* 2014). Notably, the Rotta model is consistent with the standard Langevin model (SLM) for the fluid (Pope 2000), and for this reason it is usually chosen as the standard model to be used in the hybrid Eulerian/Lagrangian pdf approach (Minier *et al.* 2014).

6. RA equations

The Fokker–Planck (FP) equation corresponding, from the pdf point of view, to the Lagrangian system of stochastic differential equations (3.6)–(3.8), (4.22), is defined in appendix C. It can be used to derive the PA equations for the particle phase by integration of the Eulerian mass density function (mdf), $F_p^E(t, \boldsymbol{x}; \boldsymbol{U}_p, \boldsymbol{\delta v}_p, \boldsymbol{U}_s)$, over the phase space:

$$\langle\alpha_p\rangle(t,\boldsymbol{x})\rho_p\langle\mathbb{O}\rangle_p(t,\boldsymbol{x}) := \int \mathbb{O}(\boldsymbol{U}_p, \boldsymbol{\delta v}_p, \boldsymbol{U}_s)F_p^E(t, \boldsymbol{x}; \boldsymbol{U}_p, \boldsymbol{\delta v}_p, \boldsymbol{U}_s)\,\mathrm{d}\boldsymbol{U}_p\,\mathrm{d}\boldsymbol{\delta v}_p\,\mathrm{d}\boldsymbol{U}_s, \tag{6.1}$$

where $\mathbb{O}$ is a generic observable attached to a discrete particle.

https://doi.org/10.1017/jfm.2018.895 Published online by Cambridge University Press

Closed RA transport equations can now be derived from the FP equation. The so-obtained RA continuity equation is the following:

$$\frac{\partial}{\partial t}(\langle\alpha_p\rangle\rho_p) + \boldsymbol{\nabla}\cdot(\langle\alpha_p\rangle\rho_p\langle\boldsymbol{U}_p\rangle) = 0. \tag{6.2}$$

The momentum equation reads

$$\langle\alpha_p\rangle\rho_p\frac{\mathrm{D}}{\mathrm{D}t}\langle\boldsymbol{U}_p\rangle = -\boldsymbol{\nabla}\cdot\langle\alpha_p\rangle\rho_p(\langle\boldsymbol{u}_p\otimes\boldsymbol{u}_p\rangle + \langle\boldsymbol{P}\rangle) + \langle\alpha_p\rangle\rho_p\left\langle\frac{\boldsymbol{U}_s-\boldsymbol{U}_p}{\tau_p}\right\rangle + \langle\alpha_p\rangle\boldsymbol{g}, \tag{6.3}$$

where $\mathrm{D}/\mathrm{D}t = \partial/\partial t + \langle\boldsymbol{U}_p\rangle\cdot\boldsymbol{\nabla}$. Second-order moments, on the other hand, give the following equations for the particle-phase Reynolds stress:

$$\begin{aligned}\langle\alpha_p\rangle\rho_p\frac{\mathrm{D}}{\mathrm{D}t}\langle\boldsymbol{u}_p\otimes\boldsymbol{u}_p\rangle = &-\boldsymbol{\nabla}\cdot(\langle\alpha_p\rangle\rho_p\langle\boldsymbol{u}_p\otimes\boldsymbol{u}_p\otimes\boldsymbol{u}_p\rangle) - \langle\alpha_p\rangle\rho_p(\langle\boldsymbol{u}_p\otimes\boldsymbol{u}_p\rangle\cdot\boldsymbol{\nabla}\langle\boldsymbol{U}_p\rangle)^{\dagger}\\ &+\frac{\langle\alpha_p\rangle\rho_p}{\tau_p}(\langle\boldsymbol{u}_s\otimes\boldsymbol{u}_p\rangle - \langle\boldsymbol{u}_p\otimes\boldsymbol{u}_p\rangle)^{\dagger} + \langle\alpha_p\rangle\rho_p\boldsymbol{\mathcal{R}}_p - \langle\alpha_p\rangle\rho_p\boldsymbol{\varepsilon}_p,\end{aligned} \tag{6.4}$$

where the redistribution is expressed by

$$\boldsymbol{\mathcal{R}}_p = -C_{Rp}\frac{\varepsilon_p}{k_p}\left(\langle\boldsymbol{u}_p\otimes\boldsymbol{u}_p\rangle - \frac{2}{3}k_p\boldsymbol{I}\right), \tag{6.5}$$

with

$$C_{Rp} = 1 + \tfrac{3}{2}C_{0p}, \tag{6.6}$$

and the dissipation tensor is closed using the Rotta model (Pope 2000),

$$\boldsymbol{\varepsilon}_p = \varepsilon_p\left[f_s\frac{\langle\boldsymbol{u}_p\otimes\boldsymbol{u}_p\rangle}{k_p} + (1-f_s)\frac{2}{3}\boldsymbol{I}\right]. \tag{6.7}$$

The transport equation for the particle-phase pressure tensor is

$$\begin{aligned}\langle\alpha_p\rangle\rho_p\frac{\mathrm{D}}{\mathrm{D}t}\langle\boldsymbol{P}\rangle \;=\; &-\boldsymbol{\nabla}\cdot[\langle\alpha_p\rangle\rho_p(\langle\boldsymbol{u}_p\otimes\boldsymbol{P}\rangle + \langle\boldsymbol{Q}\rangle)] - \langle\alpha_p\rangle\rho_p(\langle\boldsymbol{P}\rangle\cdot\boldsymbol{\nabla}\langle\boldsymbol{U}_p\rangle)^{\dagger} + \langle\alpha_p\rangle\rho_p\boldsymbol{\varepsilon}_p\\ &-\frac{2}{\tau_p}\langle\alpha_p\rangle\rho_p\langle\boldsymbol{P}\rangle + \frac{1}{2\tau_c}[(1+e)^2\langle\Theta_p\rangle\boldsymbol{I} - (1+e)(3-e)\langle\boldsymbol{P}\rangle].\end{aligned} \tag{6.8}$$

Comparing (6.4), (6.8)–(A 2), (A 3), we can see that the closed terms have been reproduced correctly in the Lagrangian pdf model, while the previously unclosed terms such as dissipation are now modelled.

Particular attention should be given to the closure of the term $\boldsymbol{\varepsilon}_p = \langle\boldsymbol{P}\cdot\boldsymbol{\nabla}\widetilde{\boldsymbol{v}}_p\rangle$, which plays the role of a sink in the equation of the particle-phase turbulent kinetic energy and of a source in the equation of the particle-phase pressure tensor. In analogy to single-phase flow, where dissipation of turbulent kinetic energy leads to viscous heating, it is modelled as a particle-phase anisotropic dissipation tensor $\boldsymbol{\varepsilon}_p$, whose trace divided by two gives the scalar particle-phase dissipation ε_p. As shown in Capecelatro *et al.* (2015) and Capecelatro, Desjardins & Fox (2016*a*), when the mean

https://doi.org/10.1017/jfm.2018.895 Published online by Cambridge University Press

mass loading is significant, the particle-phase pressure tensor is highly anisotropic due to the source term $\boldsymbol{\varepsilon}_p$ (i.e. $f_s \approx 0.93$ in (6.7)).

The transport equation of the scalar particle-phase dissipation is modelled as follows:

$$\frac{\partial \langle\alpha_p\rangle\varepsilon_p}{\partial t} + \boldsymbol{\nabla}\cdot(\langle\alpha_p\rangle\langle\boldsymbol{U}_p\rangle\varepsilon_p) = \boldsymbol{\nabla}\cdot\left[\langle\alpha_p\rangle\left(\nu_p + \frac{\nu_{p,t}}{\sigma_{\epsilon,p}}\right)\boldsymbol{\nabla}\varepsilon_p\right] - \langle\alpha_p\rangle C_{\epsilon 1p}\langle\boldsymbol{u}_p\otimes\boldsymbol{u}_p\rangle : \boldsymbol{\nabla}\langle\boldsymbol{U}_p\rangle\frac{\varepsilon_p}{k_p} - \langle\alpha_p\rangle C_{\epsilon 2p}\frac{\varepsilon_p^2}{k_p} + \langle\alpha_p\rangle\frac{C_{3p}}{\tau_p}\left(\frac{k_{fp}}{k_{f@p}}\varepsilon_f - \beta_p\varepsilon_p\right), \quad (6.9)$$

where $C_{\epsilon 1p}$, $C_{\epsilon 2p}$, C_{3p} and β_p are model parameters. Equation (6.9) differs slightly from the model in Fox (2014) because k_{fp} is known in the Lagrangian pdf model proposed here. Now that we have modelled the particle-phase dissipation, we can define a time scale for the particle phase $T_p = k_p/\varepsilon_p$ to be used in the model equation for the fluid-phase dissipation.

For the fluid-phase dissipation, we propose the following model, built with the standard single-phase fluid dissipation model equation (Pope 2000) and an additional contribution due to particle–fluid interactions:

$$\frac{\partial \langle\alpha_f\rangle\varepsilon_f}{\partial t} + \boldsymbol{\nabla}\cdot(\langle\alpha_f\rangle\langle\boldsymbol{U}_f\rangle\varepsilon_f) = \boldsymbol{\nabla}\cdot\left[\langle\alpha_f\rangle\left(\nu + \frac{\nu_t}{\sigma_\epsilon}\right)\boldsymbol{\nabla}\varepsilon_f\right] - \langle\alpha_f\rangle C_{\epsilon 1f}\langle\boldsymbol{u}_f\otimes\boldsymbol{u}_f\rangle : \boldsymbol{\nabla}\langle\boldsymbol{U}_f\rangle\frac{\varepsilon_f}{k_f} - \langle\alpha_f\rangle C_{\epsilon 2f}\frac{\varepsilon_f^2}{k_f} + \frac{\rho_p\langle\alpha_p\rangle}{\rho_f}\frac{C_{3f}}{\tau_p}\left(\frac{k_{fp}}{k_{f@p}}\varepsilon_p - \beta_f\varepsilon_f\right) + \frac{\rho_p\langle\alpha_p\rangle}{\rho_f}\frac{C_4}{\tau_p}\frac{(\langle\boldsymbol{U}_p\rangle - \langle\boldsymbol{U}_f\rangle)\cdot\langle\boldsymbol{u}_d\rangle}{2}\frac{\varepsilon_p}{k_p}, \quad (6.10)$$

where $C_{\epsilon 1f}$, $C_{\epsilon 2f}$, C_{3f}, β_f and C_4 are model constants, and $\langle\boldsymbol{u}_d\rangle = \langle\boldsymbol{U}_s\rangle - \langle\boldsymbol{U}_f\rangle$. Here, we have split the total energy rate dissipation into two contributions, arising from the energy exchange between phases (fourth term on the right-hand side), and from the drag production (last term).

The Lagrangian pdf approach is tantamount to computing the entire pdf of the variables considered in the state vector. Compared with an Eulerian moment approach, it means that more information is available. Notably, we wish to derive here the RA equations for the mean fluid velocity seen by the particles $\langle\boldsymbol{U}_s\rangle$, and for all the second-order velocity moments, $\langle\boldsymbol{u}_s\otimes\boldsymbol{u}_s\rangle$, $\langle\boldsymbol{u}_s\otimes\boldsymbol{u}_p\rangle$, which cannot be accessed in present two-fluid models. We can obtain the RA equations starting from the transport equation of the Eulerian mdf F_p^E (C 1):

$$\langle\alpha_p\rangle\rho_p\frac{\mathrm{D}}{\mathrm{D}t}\langle\boldsymbol{U}_s\rangle = -\boldsymbol{\nabla}\cdot(\langle\alpha_p\rangle\rho_p\langle\boldsymbol{u}_s\otimes\boldsymbol{u}_p\rangle) + \langle\alpha_p\rangle\rho_p\left[-\frac{\langle\alpha_f\rangle}{\rho_f}\boldsymbol{\nabla}\langle p_f\rangle + (\boldsymbol{\nabla}\langle\boldsymbol{U}_f\rangle)\cdot(\langle\boldsymbol{U}_p\rangle - \langle\boldsymbol{U}_f\rangle) + \boldsymbol{G}\cdot(\langle\boldsymbol{U}_s\rangle - \langle\boldsymbol{U}_f\rangle) + \boldsymbol{g}\right] - \langle\alpha_p\rangle\rho_p\varphi\left(\frac{\langle\boldsymbol{U}_s - \boldsymbol{U}_p\rangle}{\tau_p}\right), \quad (6.11)$$

where $\mathrm{D}/\mathrm{D}t = \partial/\partial t + \langle\boldsymbol{U}_p\rangle\cdot\boldsymbol{\nabla}$.

https://doi.org/10.1017/jfm.2018.895 Published online by Cambridge University Press

For the second-order moments we obtain

$$\begin{aligned}\langle\alpha_p\rangle\rho_p\frac{\mathrm{D}}{\mathrm{D}t}\langle\boldsymbol{u}_s\otimes\boldsymbol{u}_p\rangle &= -\boldsymbol{\nabla}\cdot[\langle\alpha_p\rangle\rho_p(\langle\boldsymbol{u}_s\otimes\boldsymbol{u}_p\otimes\boldsymbol{u}_p\rangle+\langle\boldsymbol{u}_s\otimes\delta\boldsymbol{v}_p\otimes\delta\boldsymbol{v}_p\rangle)]\\ &\quad-\langle\alpha_p\rangle\rho_p(\langle\boldsymbol{u}_s\otimes\boldsymbol{u}_p\rangle\cdot\boldsymbol{\nabla}\langle\boldsymbol{U}_p\rangle^T)-\langle\alpha_p\rangle\rho_p[(\langle\boldsymbol{u}_p\otimes\boldsymbol{u}_p\rangle+\langle\delta\boldsymbol{v}_p\otimes\delta\boldsymbol{v}_p\rangle)\cdot\boldsymbol{\nabla}\langle\boldsymbol{U}_s\rangle^T]\\ &\quad+\langle\alpha_p\rangle\rho_p\boldsymbol{G}\cdot\langle\boldsymbol{u}_s\otimes\boldsymbol{u}_p\rangle^T+\langle\alpha_p\rangle\rho_p\varphi\frac{\langle\boldsymbol{u}_p\otimes\boldsymbol{u}_p\rangle-\langle\boldsymbol{u}_s\otimes\boldsymbol{u}_p\rangle}{\tau_p}\\ &\quad-\langle\alpha_p\rangle\rho_p\frac{1}{T_{Lp}}\langle\boldsymbol{u}_p\otimes\boldsymbol{u}_s\rangle+\langle\alpha_p\rangle\rho_p\frac{\langle\boldsymbol{u}_s\otimes\boldsymbol{u}_s\rangle-\langle\boldsymbol{u}_p\otimes\boldsymbol{u}_s\rangle}{\tau_p}\end{aligned}\tag{6.12}$$

and

$$\begin{aligned}\langle\alpha_p\rangle\rho_p\frac{\mathrm{D}}{\mathrm{D}t}\langle\boldsymbol{u}_s\otimes\boldsymbol{u}_s\rangle &= -\boldsymbol{\nabla}\cdot(\langle\alpha_p\rangle\rho_p\langle\boldsymbol{u}_s\otimes\boldsymbol{u}_s\otimes\boldsymbol{u}_s\rangle)-\langle\alpha_p\rangle\rho_p(\langle\boldsymbol{u}_s\otimes\boldsymbol{u}_s\rangle\cdot\boldsymbol{\nabla}\langle\boldsymbol{U}_s\rangle)^\dagger\\ &\quad+\langle\alpha_p\rangle\rho_p(\boldsymbol{G}\cdot\langle\boldsymbol{u}_s\otimes\boldsymbol{u}_s\rangle)^\dagger+\langle\alpha_p\rangle\rho_p\varphi\frac{\langle\boldsymbol{u}_s\otimes\boldsymbol{u}_p\rangle^\dagger-2\langle\boldsymbol{u}_s\otimes\boldsymbol{u}_s\rangle}{\tau_p}+\langle\alpha_p\rangle\rho_p\langle\boldsymbol{B}_s\boldsymbol{B}_s^{\mathrm{T}}\rangle.\end{aligned}\tag{6.13}$$

Eulerian transport equations for the cross-correlations $\langle\boldsymbol{u}_p\otimes\delta\boldsymbol{v}_p\rangle$ and $\langle\boldsymbol{u}_s\otimes\delta\boldsymbol{v}_p\rangle$ could also be written to demonstrate that $\delta\boldsymbol{v}_p$ is uncorrelated with the other variables. Also, it is important to note that these moment equations are, in general, not closed (e.g. the turbulent fluxes involve the third-order moments). However, for statistically homogeneous flows such as particle-laden isotropic turbulence (Elghobashi 1994; Sundaram & Collins 1999; Février *et al.* 2005) and CIT (Capecelatro *et al.* 2015), the spatial gradients (except for fluid pressure, whose gradient is constant) are zero, and a closed set of moment equations results.

7. Statistically homogeneous equations

7.1. *Particle phase*

For statistically homogeneous flow, the Eulerian equations corresponding to the stochastic equation system (3.6)–(3.8) and (4.22) are the following:

$$\frac{\mathrm{d}\langle\boldsymbol{U}_p\rangle}{\mathrm{d}t}=\frac{1}{\tau_p}\langle\boldsymbol{U}_s-\boldsymbol{U}_p\rangle+\boldsymbol{g},\tag{7.1}$$

$$\langle\delta\boldsymbol{v}_p\rangle=0,\tag{7.2}$$

$$\frac{\mathrm{d}\langle\boldsymbol{U}_s\rangle}{\mathrm{d}t}=-\frac{\langle\alpha_f\rangle}{\rho_f}\boldsymbol{\nabla}\langle p_f\rangle+\boldsymbol{G}\cdot(\langle\boldsymbol{U}_s\rangle-\langle\boldsymbol{U}_f\rangle)+\frac{\varphi}{\tau_p}\langle\boldsymbol{U}_p-\boldsymbol{U}_s\rangle+\boldsymbol{g}.\tag{7.3}$$

The particle-phase pressure tensor, $\langle\boldsymbol{P}\rangle=\langle\delta\boldsymbol{v}_p\otimes\delta\boldsymbol{v}_p\rangle$, is found from

$$\frac{\mathrm{d}\langle\boldsymbol{P}\rangle}{\mathrm{d}t}=\boldsymbol{\mathcal{P}}_P+\boldsymbol{\varepsilon}_p-\frac{2}{\tau_p}\langle\boldsymbol{P}\rangle+\frac{1}{2\tau_c}[(1+e)^2\langle\Theta_p\rangle\boldsymbol{I}-(1+e)(3-e)\langle\boldsymbol{P}\rangle],\tag{7.4}$$

where $\langle\Theta_p\rangle=(1/3)\mathrm{Trace}(\langle\boldsymbol{P}\rangle)$ and the production term due to mean velocity gradients is

$$\boldsymbol{\mathcal{P}}_P=-(\langle\boldsymbol{P}\rangle\cdot\boldsymbol{\nabla}\langle\boldsymbol{U}_p\rangle)^\dagger.\tag{7.5}$$

For the particle-phase Reynolds-stress tensor, we obtain

$$\frac{\mathrm{d}\langle\boldsymbol{u}_p\otimes\boldsymbol{u}_p\rangle}{\mathrm{d}t}=\boldsymbol{\mathcal{P}}_p+\boldsymbol{\mathcal{R}}_p-\boldsymbol{\varepsilon}_p.\tag{7.6}$$

https://doi.org/10.1017/jfm.2018.895 Published online by Cambridge University Press

The redistribution term is expressed as

$$\mathcal{R}_p = -C_{Rp}\frac{\varepsilon_p}{k_p}\left(\langle \boldsymbol{u}_p \otimes \boldsymbol{u}_p\rangle - \frac{2}{3}k_p\boldsymbol{I}\right). \tag{7.7}$$

The production term in (7.6) is defined by $\mathcal{P}_p = \mathcal{P}_{Sp} + \mathcal{P}_{Dp}$ where $\mathcal{P}_{Sp}$ is the mean-shear-production term, given by

$$\mathcal{P}_{Sp} = -(\langle \boldsymbol{u}_p \otimes \boldsymbol{u}_p\rangle \cdot \boldsymbol{\nabla}\langle \boldsymbol{U}_p\rangle)^{\dagger}, \tag{7.8}$$

and $\mathcal{P}_{Dp}$ is the drag-production term, given by

$$\mathcal{P}_{Dp} = \frac{1}{\tau_p}(\langle \boldsymbol{u}_s \otimes \boldsymbol{u}_p\rangle^{\dagger} - 2\langle \boldsymbol{u}_p \otimes \boldsymbol{u}_p\rangle). \tag{7.9}$$

The fluid-seen Reynolds-stress tensor is found from

$$\frac{\mathrm{d}\langle \boldsymbol{u}_s \otimes \boldsymbol{u}_s\rangle}{\mathrm{d}t} = \mathcal{P}_s + (\boldsymbol{G}\cdot\langle \boldsymbol{u}_s \otimes \boldsymbol{u}_s\rangle)^{\dagger} + \langle \boldsymbol{B}_s\boldsymbol{B}_s^{\mathrm{T}}\rangle, \tag{7.10}$$

where $\boldsymbol{B}_s$ is the diffusion matrix in (4.22) and $k_{f@p} = (1/2)\langle(\boldsymbol{U}_s - \langle \boldsymbol{U}_f\rangle)\cdot(\boldsymbol{U}_s - \langle \boldsymbol{U}_f\rangle)\rangle$. The production term in (7.10) is defined by $\mathcal{P}_s = \mathcal{P}_{Ss} + \mathcal{P}_{Ds}$ where $\mathcal{P}_{Ss}$ is the mean-shear-production term, given by

$$\mathcal{P}_{Ss} = -(\langle \boldsymbol{u}_s \otimes \boldsymbol{u}_s\rangle \cdot \boldsymbol{\nabla}\langle \boldsymbol{U}_s\rangle)^{\dagger}, \tag{7.11}$$

and $\mathcal{P}_{Ds}$ is the drag-production term, given by

$$\mathcal{P}_{Ds} = \frac{\varphi}{\tau_p}(\langle \boldsymbol{u}_s \otimes \boldsymbol{u}_p\rangle^{\dagger} - 2\langle \boldsymbol{u}_s \otimes \boldsymbol{u}_s\rangle). \tag{7.12}$$

The fluid–particle covariance Reynolds-stress tensor is found from

$$\frac{\mathrm{d}\langle \boldsymbol{u}_s \otimes \boldsymbol{u}_p\rangle}{\mathrm{d}t} = \mathcal{P}_{sp} + \boldsymbol{G}\cdot\langle \boldsymbol{u}_s \otimes \boldsymbol{u}_p\rangle^{T} - \frac{1}{T_{Lp}}\langle \boldsymbol{u}_p \otimes \boldsymbol{u}_s\rangle, \tag{7.13}$$

where $k_{fp} = (1/2)\langle \boldsymbol{u}_s \cdot \boldsymbol{u}_p\rangle$. The production term in (7.13) is defined by $\mathcal{P}_{sp} = \mathcal{P}_{Ssp} + \mathcal{P}_{Dsp}$ where $\mathcal{P}_{Ssp}$ is the mean-shear-production term, given by

$$\mathcal{P}_{Ssp} = -\langle \boldsymbol{u}_s \otimes \boldsymbol{u}_p\rangle \cdot \boldsymbol{\nabla}\langle \boldsymbol{U}_p\rangle^{\mathrm{T}} - (\langle \boldsymbol{u}_p \otimes \boldsymbol{u}_p\rangle + \langle \boldsymbol{P}\rangle)\cdot\boldsymbol{\nabla}\langle \boldsymbol{U}_s\rangle^{\mathrm{T}}, \tag{7.14}$$

and $\mathcal{P}_{Dsp}$ is the drag-production term, given by

$$\mathcal{P}_{Dsp} = \frac{1}{\tau_p}(\langle \boldsymbol{u}_s \otimes \boldsymbol{u}_s\rangle - \langle \boldsymbol{u}_p \otimes \boldsymbol{u}_s\rangle) + \frac{\varphi}{\tau_p}(\langle \boldsymbol{u}_p \otimes \boldsymbol{u}_p\rangle - \langle \boldsymbol{u}_s \otimes \boldsymbol{u}_p\rangle). \tag{7.15}$$

The particle-phase dissipation equation becomes

$$\frac{\mathrm{d}\varepsilon_p}{\mathrm{d}t} = (C_{\epsilon 1p}\mathcal{P}_{Sp} - C_{\epsilon 2p}\varepsilon_p)\frac{\varepsilon_p}{k_p} + \frac{C_{3p}}{\tau_p}\left(\frac{k_{fp}}{k_{f@p}}\varepsilon_f - \beta_p\varepsilon_p\right). \tag{7.16}$$

Finally, all the fluid-phase quantities are obtained through the RA equations presented in § 7.3.

https://doi.org/10.1017/jfm.2018.895 Published online by Cambridge University Press

7.2. *Simplified model for particle phase*

We propose here a simplified model for the particle phase, where collisions between particles are neglected and only the total particle velocity is modelled, thus losing information about its decomposition into the correlated and uncorrelated parts. In particular, this corresponds to assuming that the particle velocity coincides with the correlated part, i.e. $\boldsymbol{V}_p = \boldsymbol{U}_p$. The resulting set of stochastic differential equations (SDEs) for the simplified model is

$$\left.\begin{aligned}
\mathrm{d}x_{p,i}(t) &= V_{p,i}\,\mathrm{d}t,\\
\mathrm{d}V_{p,i}(t) &= \frac{U_{s,i}-V_{p,i}}{\tau_p}\,\mathrm{d}t + g_i\,\mathrm{d}t,\\
\mathrm{d}U_{s,i}(t) &= -\frac{\langle\alpha_f\rangle}{\rho_f}\frac{\partial\langle p_f\rangle}{\partial x_i}\,\mathrm{d}t - \frac{1}{T^*_{L,i}}(U_{s,i}-\langle U_{f,i}\rangle)\,\mathrm{d}t - \varphi\left(\frac{U_{s,i}-V_{p,i}}{\tau_p}\right)\mathrm{d}t + g_i\,\mathrm{d}t\\
&\quad + \left[\varepsilon_f\left(C_{0f}b_i\frac{\tilde{k}_f}{k_f}+\frac{2}{3}\left(b_i\frac{\tilde{k}_f}{k_f}-1\right)\right) + 2\varphi\frac{\langle V_{p,i}-U_{s,i}\rangle}{\tau_p}(\langle U_{s,i}\rangle-\langle U_{f,i}\rangle)\right.\\
&\quad \left. - 2\frac{\langle\alpha_p\rangle}{\langle\alpha_f\rangle\rho_f}\frac{\partial\langle p_f\rangle}{\partial x_i}(\langle U_{s,i}\rangle-\langle U_{f,i}\rangle)\right]^{1/2}\mathrm{d}W_{s,i},
\end{aligned}\right\} \tag{7.17}$$

where all of the parameters were defined in the complete model above.

The corresponding Eulerian RA equations for statistically homogeneous flow are

$$\frac{\mathrm{d}\langle\boldsymbol{V}_p\rangle}{\mathrm{d}t} = \frac{1}{\tau_p}\langle\boldsymbol{U}_s-\boldsymbol{V}_p\rangle + \boldsymbol{g}, \tag{7.18}$$

$$\frac{\mathrm{d}\langle\boldsymbol{U}_s\rangle}{\mathrm{d}t} = -\frac{\langle\alpha_f\rangle}{\rho_f}\boldsymbol{\nabla}\langle p_f\rangle - \frac{1}{\boldsymbol{T}^*_L}\circ(\langle\boldsymbol{U}_s\rangle-\langle\boldsymbol{U}_f\rangle) + \frac{\varphi}{\tau_p}\langle\boldsymbol{V}_p-\boldsymbol{U}_s\rangle + \boldsymbol{g}, \tag{7.19}$$

where the $\circ$ symbol denotes an element-by-element product. For the second-order moments, we obtain

$$\frac{\mathrm{d}\langle\boldsymbol{v}_p\otimes\boldsymbol{v}_p\rangle}{\mathrm{d}t} = \boldsymbol{\mathcal{P}}_{Vp} + \frac{1}{\tau_p}(\langle\boldsymbol{u}_s\otimes\boldsymbol{v}_p\rangle^{\dagger} - 2\langle\boldsymbol{v}_p\otimes\boldsymbol{v}_p\rangle), \tag{7.20}$$

$$\begin{aligned}
\frac{\mathrm{d}\langle\boldsymbol{u}_s\otimes\boldsymbol{v}_p\rangle}{\mathrm{d}t} &= \boldsymbol{\mathcal{P}}_{Vsp} - \frac{1}{\boldsymbol{T}^*_L}\circ\langle\boldsymbol{u}_s\otimes\boldsymbol{v}_p\rangle + \frac{1}{\tau_p}(\langle\boldsymbol{u}_s\otimes\boldsymbol{u}_s\rangle - \langle\boldsymbol{v}_p\otimes\boldsymbol{u}_s\rangle)\\
&\quad + \frac{\varphi}{\tau_p}(\langle\boldsymbol{v}_p\otimes\boldsymbol{v}_p\rangle - \langle\boldsymbol{u}_s\otimes\boldsymbol{v}_p\rangle),
\end{aligned} \tag{7.21}$$

$$\frac{\mathrm{d}\langle\boldsymbol{u}_s\otimes\boldsymbol{u}_s\rangle}{\mathrm{d}t} = \boldsymbol{\mathcal{P}}_{Ss} - \frac{2}{\boldsymbol{T}^*_L}\circ\langle\boldsymbol{u}_s\otimes\boldsymbol{u}_s\rangle + \langle\boldsymbol{B}_s\boldsymbol{B}_s^{\mathrm{T}}\rangle + \frac{\varphi}{\tau_p}(\langle\boldsymbol{u}_s\otimes\boldsymbol{v}_p\rangle^{\dagger} - 2\langle\boldsymbol{u}_s\otimes\boldsymbol{u}_s\rangle). \tag{7.22}$$

The mean-shear-production terms are

$$\boldsymbol{\mathcal{P}}_{Vp} = -(\langle\boldsymbol{v}_p\otimes\boldsymbol{v}_p\rangle\cdot\boldsymbol{\nabla}\langle\boldsymbol{V}_p\rangle)^{\dagger} \tag{7.23}$$

and

$$\boldsymbol{\mathcal{P}}_{Vsp} = -\langle\boldsymbol{u}_s\otimes\boldsymbol{v}_p\rangle\cdot\boldsymbol{\nabla}\langle\boldsymbol{V}_p\rangle^{\mathrm{T}} - \langle\boldsymbol{v}_p\otimes\boldsymbol{v}_p\rangle\cdot\boldsymbol{\nabla}\langle\boldsymbol{U}_s\rangle^{\mathrm{T}}. \tag{7.24}$$

This model is similar to the model previously proposed by Minier *et al.* (2004) and Peirano *et al.* (2006) for the fluid velocity seen by the particles, but with a modified diffusion term, as discussed in detail in § 4.1. Furthermore, both models have the same dilute limit ($\langle\alpha_f\rangle = 1$).

https://doi.org/10.1017/jfm.2018.895 Published online by Cambridge University Press

7.3. *Fluid phase*

The Eulerian RA equation describing the fluid-phase mass balance for a statistically homogeneous flow reduces to

$$\frac{\mathrm{d}\langle\alpha_f\rangle}{\mathrm{d}t} = 0, \tag{7.25}$$

i.e. $\langle\alpha_f\rangle$ is constant. The fluid-phase velocity and Reynolds stresses are found from

$$\frac{\mathrm{d}\langle\boldsymbol{U}_f\rangle}{\mathrm{d}t} = -\frac{1}{\rho_f}\boldsymbol{\nabla}\langle p_f\rangle + \frac{\varphi}{\tau_p}\langle\boldsymbol{U}_p - \boldsymbol{U}_s\rangle + \boldsymbol{g}, \tag{7.26}$$

and

$$\frac{\mathrm{d}\langle\boldsymbol{u}_f\otimes\boldsymbol{u}_f\rangle}{\mathrm{d}t} = \boldsymbol{\mathcal{P}}_f - C_{Rf}\frac{\varepsilon_f}{k_f}\left(\langle\boldsymbol{u}_f\otimes\boldsymbol{u}_f\rangle - \frac{2}{3}k_f\boldsymbol{I}\right) - C_{2f}\left(\boldsymbol{\mathcal{P}}_{Sf} - \frac{2}{3}\mathcal{P}_{Sf}\boldsymbol{I}\right) - \frac{2}{3}\varepsilon_f\boldsymbol{I}, \tag{7.27}$$

where $k_f = (1/2)\langle\boldsymbol{u}_f\cdot\boldsymbol{u}_f\rangle$. The production term is $\boldsymbol{\mathcal{P}}_f = \boldsymbol{\mathcal{P}}_{Sf} + \boldsymbol{\mathcal{P}}_{Df}$ where $\boldsymbol{\mathcal{P}}_{Sf}$ is the mean-shear-production term, given by

$$\boldsymbol{\mathcal{P}}_{Sf} = -(\langle\boldsymbol{u}_f\otimes\boldsymbol{u}_f\rangle\cdot\boldsymbol{\nabla}\langle\boldsymbol{U}_f\rangle)^{\dagger}, \tag{7.28}$$

and $\boldsymbol{\mathcal{P}}_{Df}$ is the drag-production term, given by

$$\boldsymbol{\mathcal{P}}_{Df} = \frac{\varphi}{\tau_p}[\langle\boldsymbol{u}_s\otimes(\boldsymbol{u}_p-\boldsymbol{u}_s)\rangle + \langle\boldsymbol{U}_s-\boldsymbol{U}_f\rangle\otimes\langle\boldsymbol{U}_p-\boldsymbol{U}_s\rangle]^{\dagger}. \tag{7.29}$$

In (7.27), C_{Rf} is the Rotta constant for the redistribution (Pope 2000), and $\mathcal{P}_{Sf} = (1/2)\mathrm{trace}(\boldsymbol{\mathcal{P}}_{Sf})$.

The fluid-phase dissipation equation becomes

$$\frac{\mathrm{d}\varepsilon_f}{\mathrm{d}t} = \left(C_{\epsilon 1f}\mathcal{P}_{Sf} - C_{\epsilon 2f}\varepsilon_f\right)\frac{\varepsilon_f}{k_f} + C_{3f}\frac{\varphi}{\tau_p}\left(\frac{k_{fp}}{k_{f@p}}\varepsilon_p - \beta_f\varepsilon_f\right) + C_4\frac{\varepsilon_p}{k_p}\mathcal{P}_D, \tag{7.30}$$

with

$$\mathcal{P}_D = \frac{\varphi}{\tau_p}\frac{\langle\boldsymbol{U}_s-\boldsymbol{U}_f\rangle\cdot\langle\boldsymbol{U}_p-\boldsymbol{U}_f\rangle}{2}. \tag{7.31}$$

If the RA equations for the fluid phase are coupled with the simplified model described in § 7.2, $\boldsymbol{U}_p$ must be replaced with $\boldsymbol{V}_p$. Moreover, the particle-phase Lagrangian time scale k_p/ε_p is not specified, and it is thus replaced by a fluid time scale through a proportionality constraint:

$$\frac{\varepsilon_p}{k_p} = \alpha\frac{\varepsilon_f}{k_{f@p}}. \tag{7.32}$$

Now, substituting (7.32) in (7.30) and incorporating α in the model constants, gives the following equation for dissipation:

$$\frac{\mathrm{d}\varepsilon_f}{\mathrm{d}t} = \left(C_{\epsilon 1f}\mathcal{P}_{Sf} - C_{\epsilon 2f}\varepsilon_f\right)\frac{\varepsilon_f}{k_f} + C_{3f}\frac{\varphi}{\tau_p}\left(\frac{k_p}{k_{f@p}}k_{fp} - \beta_f k_{f@p}\right)\frac{\varepsilon_f}{k_{f@p}} + C_4\frac{\varepsilon_f}{k_{f@p}}\mathcal{P}_D. \tag{7.33}$$

The values of C_{3f} and C_4 in (7.33) may need to be adjusted as compared to (7.30) to account for the alternative time scale.

https://doi.org/10.1017/jfm.2018.895 Published online by Cambridge University Press

8. Numerical results

We present three spatially homogeneous examples of increasing complexity: (i) isotropic turbulence with one-way coupling, (Février *et al.* 2005), (ii) isotropic decaying (Sundaram & Collins 1999) and sheared turbulence (Ahmed & Elghobashi 2000) with two-way coupling, and (iii) gravity-driven CIT (Capecelatro *et al.* 2015). The first example is aimed at appraising the partitioning of the particle kinetic energy, the second at testing the dynamics in the absence/presence of shear production (i.e. $\mathcal{P}_{Sf}$) without a mean velocity difference, and the third, and most important one, at validating the model for production due to a mean velocity difference (i.e. (7.31)).

8.1. *Homogeneous isotropic turbulence*

In order to illustrate the effectiveness of the decomposition of the particle velocity, we apply the models developed for the particle phase to the homogeneous isotropic turbulence simulations of Février *et al.* (2005) for non-collisional particles. For this example, the mean velocities $\boldsymbol{U}_p$, $\boldsymbol{U}_f$, $\boldsymbol{U}_s$ are null, and $\varphi = 0$. At a first glance it may appear odd to compare the results of a model developed for collisional flows to DNS data for non-collisional particles. However, the crucial point for the modelling is the correlation between the fluid and particle velocities as captured by k_f and k_p, respectively. The applicability of the proposed models to non-collisional flows depends on the model used for turbulent dissipation, since the relative balance between k_p and Θ_p is determined by ε_p, for both dilute and dense flows. The scope of this section is thus to verify if in the dilute case, where collisions do not play any role, energy budgets are well predicted. The point-particle DNS simulations of Février *et al.* (2005) use one-way coupling with stationary fluid turbulence, and a particle-Reynolds-number-dependent drag coefficient f_D (instead of a constant τ_p). Therefore, the drag time scale is Stokes-number-dependent, and only qualitative comparisons can be made.

When a cloud of particles is put into a box filled with a homogeneous, isotropic turbulent flow and thus is agitated by the fluid turbulence, after a transient period, the statistics of particle velocities will reach equilibrium values. These limit values are of course functions of the (constant) statistics of the fluid (its mean kinetic energy, the Lagrangian time scale, among others). The relations giving the equilibrium values in terms of the fluid statistics are called the Tchen's relations. They were first obtained by Tchen (1947) and later reformulated by Hinze (1975). In Tchen or Hinze's works, the determination of the equilibrium values was obtained through spectral analysis and manipulation of the fluid and particle energy spectra, where the fluid spectrum is assumed to have an exponential form. This derivation can be cumbersome and the physical meaning of the exponential form is not obvious. On the other hand, the same relations are derived from the Lagrangian pdf model in a straightforward way.

In forced, homogeneous, isotropic turbulence without body forces, all mean velocities are zero and the Reynolds-stress and particle-phase pressure tensors are isotropic. Moreover, $k_{f@p} = k_f$. With one-way coupling and fixed k_f and ε_f, the relevant moment equations from the complete model for the particle phase reduce to

$$\frac{\mathrm{d}k_p}{\mathrm{d}t} = \frac{2}{\tau_p}(k_{fp} - k_p) - \varepsilon_p, \tag{8.1a}$$

$$\frac{3}{2}\frac{\mathrm{d}\langle\Theta_p\rangle}{\mathrm{d}t} = -\frac{3\langle\Theta_p\rangle}{\tau_p} + \varepsilon_p, \tag{8.1b}$$

$$\frac{\mathrm{d}k_{fp}}{\mathrm{d}t} = -\left(\frac{1}{T_{Lf}} + \frac{1}{T_{Lp}}\right)k_{fp} + \frac{1}{\tau_p}(k_f - k_{fp}), \tag{8.1c}$$

https://doi.org/10.1017/jfm.2018.895 Published online by Cambridge University Press

$$\frac{\mathrm{d}\varepsilon_p}{\mathrm{d}t} = -C_{\epsilon 2p}\frac{\varepsilon_p^2}{k_p} + \frac{C_{3p}}{\tau_p}\left(\frac{k_{fp}}{k_f}\varepsilon_f - \beta_p\varepsilon_p\right), \tag{8.1d}$$

where T_{Lf} is given by (4.6) and T_{Lp} by (3.9). After a transient period, all the statistics reach their steady-state values. This yields

$$2\frac{k_{fp}-k_p}{\tau_p} - \varepsilon_p = 0, \tag{8.2a}$$

$$-\frac{3\langle\Theta_p\rangle}{\tau_p} + \varepsilon_p = 0, \tag{8.2b}$$

$$\frac{k_f}{\tau_p} - \left(\frac{1}{\tau_p} + \frac{1}{T_{Lf}} + \frac{1}{T_{Lp}}\right)k_{fp} = 0, \tag{8.2c}$$

$$St_p^2 - \frac{C_{3p}}{C_{\epsilon 2p}}\left(\frac{k_{fp}}{k_p}St_f - \beta_p St_p\right) = 0, \tag{8.2d}$$

where $St_p = \tau_p\varepsilon_p/k_p$ and $St_f = \tau_p\varepsilon_f/k_f$. Summing (8.2*a*) and (8.2*b*) then yields

$$k_{fp} = \kappa_p, \tag{8.3}$$

which can be used together with (8.2*c*) to obtain a Tchen-like relation:

$$\kappa_p = \frac{1}{1+\tau_p/T_L'}k_f, \tag{8.4}$$

with $C_0 = C_{0p} = C_{0f}$ and

$$\frac{1}{T_L'} = \frac{1}{T_{Lf}} + \frac{1}{T_{Lp}} = \left(\frac{1}{2} + \frac{3}{4}C_0\right)\left(\frac{\varepsilon_f}{k_f} + \frac{\varepsilon_p}{k_p}\right). \tag{8.5}$$

Here, τ_p/T_L' is an effective integral-scale Stokes number for the particles. Furthermore, St_p is constant, and can be related to St_f using (8.2*a*) and (8.2*d*). With $\beta_p = 1$, this relation depends only on the parameter ratio $C_{3p}/C_{\epsilon 2p}$, and thus $St_p = St_f$ when $C_{3p} = 2C_{\epsilon 2p}$. Note that the value of St_p controls the ratio $k_p/\kappa_p = 2/(2+St_p)$ and, as expected, all of the particle-phase kinetic energy is spatially correlated when $St_p = 0$.

Février *et al.* (2005) presented time-dependent DNS results of particle-laden homogeneous and isotropic turbulence for $St_f = 0.81$ and $\varphi = 0$, for three sets of initial conditions: (i) $\kappa_p = k_{fp} = 1$, $k_p = 1$, (ii) $\kappa_p = k_{fp} = 0$, $k_p = 0$, and (iii) $\kappa_p = 0.83$, $k_p = k_{fp} = 0$. We reproduced the same cases by solving the dimensionless forms of system (8.1) with the following values of the model constants: $C_0 = 1$, $C_{\epsilon 2p} = 1.92$, $C_{3p} = 3.5$ and $\beta_p = 1$. For consistency with k_p, ε_p is initially set to zero when $k_p = 0$ and for case (i) the initial value of dissipation is $\varepsilon_p = 2$. Figure 1(*a*) shows the time evolution of κ_p, k_p and Θ_p obtained with the full model for the three different sets of considered initial conditions, while the evolution of κ_p obtained with the simplified model for the same cases is reported in figure 1(*b*). Moreover, figure 1(*c*) shows the same quantities as in figure 1(*a*) obtained with the model proposed in Fox (2014) and figure 1(*d*) the results of the DNS of Février *et al.* (2005). In all cases, after a transient a steady state is reached, as expected. It can be seen how in DNS the total particle kinetic energy is distributed in the correlated part and in the uncorrelated granular temperature. This energy partition is satisfactorily captured by our complete model as well as by the model proposed in Fox (2014). Clearly, the simplified model can only give the total energy κ_p, which is however in good agreement with that of DNS and of more complete models. The transient behaviour is also in very good qualitative agreement with that obtained in DNS.

https://doi.org/10.1017/jfm.2018.895 Published online by Cambridge University Press

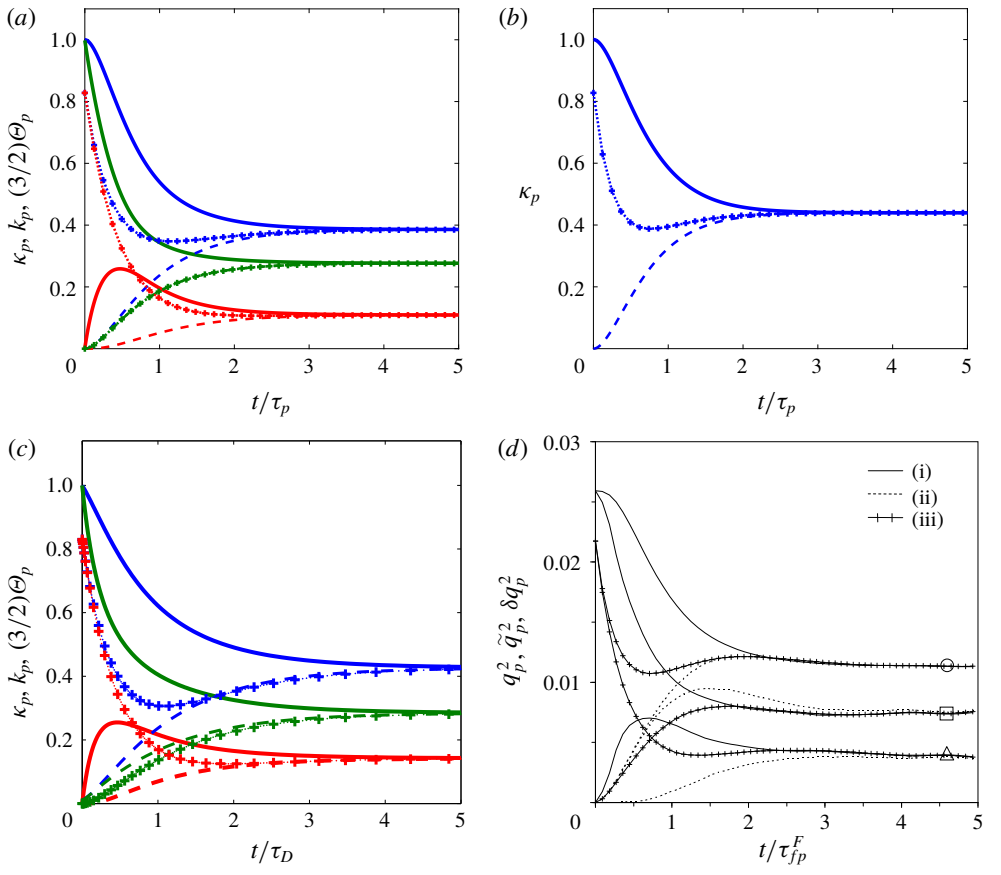


FIGURE 1. (Colour online) Time evolution of the dimensionless particle-phase energy components for $St_f = 0.81$. The curves correspond to the three considered sets of initial conditions: case (i) solid lines, (ii) dashed lines and (iii) + line. κ_p is plotted in blue, k_p in green and $(3/2)\Theta_p$ in red. (*a*) Simulations with the complete particle model (8.1). (*b*) Simulations carried out with the simplified particle model (7.17) with $C_0 = 2.1$. Only total kinetic energy κ_p is computed. (*c*) Results from Fox (2014) with the same initial conditions as in (*a*). (*d*) Results of point-particle DNS from figure 8 of Février *et al.* (2005), where the results are in dimensional form. The notation in Février *et al.* (2005) is $q_p^2 = \kappa_p$, $\widetilde{q}_p^2 = k_p$, $\delta q_p^2 = (3/2)\Theta_p$ and $\tau_{fp}^F \propto \tau_D$.

8.2. *Decaying and homogeneous-shear flow*

In this section we focus on the particle–turbulence interactions in homogeneous flows, and, in particular, on the cases simulated by DNS in Sundaram & Collins (1999) for decaying turbulence and in Ahmed & Elghobashi (2000) for homogeneous-shear flows. For these examples, the mean velocities $\boldsymbol{U}_p, \boldsymbol{U}_f, \boldsymbol{U}_s$ are null. In both cases the particle-phase volume fraction is such that two-way interactions need to be considered: flow modification by non-collisional point particles reveals a non-trivial dependence on the particle Stokes number and mass loading φ. It is thus interesting to verify if our model is able to reproduce such physics and if the same dependences on the particle Stokes number are found.

https://doi.org/10.1017/jfm.2018.895 Published online by Cambridge University Press

The Eulerian RA equations describing the fluid and particle phases for the considered cases have been shown in § 7. In particular, in the shear flow case a constant shear is present $\mathcal{S}_f = \partial\langle U_{f,1}\rangle/\partial x_2$, while $\mathcal{S}_f = 0$ in decaying turbulence. Gravity and collisions are not considered in these test cases. Note that when $\mathcal{S}_f$ is null (i.e. decaying turbulence), all second-order tensors will be isotropic so that only their traces are needed. Otherwise the non-zero components of the second-order moments are $(i, j) = (1, 1), (1, 2), (2, 1), (2, 2), (3, 3)$.

The mean gradients for the particle phase and the fluid seen by particles obey

$$\frac{\mathrm{d}\mathcal{S}_p}{\mathrm{d}t} = \frac{1}{\tau_p}(\mathcal{S}_s - \mathcal{S}_p), \tag{8.6a}$$

$$\frac{\mathrm{d}\mathcal{S}_s}{\mathrm{d}t} = \frac{1}{\tau_p}(\mathcal{S}_f - \mathcal{S}_s). \tag{8.6b}$$

In the following, the particle-phase velocity is initially the same as the fluid-phase velocity such that $\mathcal{S}_p(t) = \mathcal{S}_s(t) = \mathcal{S}_f$ and thus system (8.6) is not needed.

It is worth noting that, even in these simple flow conditions, the model still retains some of its features, as, for instance, the distinction between the fluid kinetic energy and the fluid–particle velocity correlation, which can be computed from Lagrangian quantities by averaging, i.e. $k_{fp} = (1/2)\langle u_{p,k}u_{s,k}\rangle$, while in Eulerian models that do not account for the fluid seen by the particles (see Fox (2014)), it is modelled as $k_{fp} = (k_f k_p)^{1/2}$. Moreover, it should be remarked that only a part of the crossing-trajectory effect is taken into account, that is, when there is a mean drift, and thus a mean relative velocity between fluid and particles. This means that in the case that we are testing, the modified Lagrangian time scale equals the fluid Lagrangian time scale, $T_L^* = T_L$, for all Stokes numbers. Conversely, particle inertia should affect the Lagrangian time scale of the fluid velocity seen by the particles. In particular, if we consider the limit cases, we have two situations: particles with very low inertia, i.e. $\tau_p/T_L \ll 1$, follow almost exactly the fluid, yielding $T_L^* = T_L$ for the fluid velocity seen. Particles with high inertia, i.e. $\tau_p/T_L \gg 1$, are nearly at a standstill with respect to the fluid and therefore, the fluid velocity seen time scale is approximately the Eulerian time scale, $T_L^* = T_E$. This inconsistency has already been pointed out by Pozorski & Minier (1998), and, even if it can be neglected in flows where a mean drift drives the particles, becoming secondary, here it is of crucial importance, especially if we are interested in finding the trends of the decay rate with respect to particle inertia. For this reason we propose to add a Stokes dependence in $C_{\epsilon 2}$ of the kind $C_{\epsilon 2} = C(1 - \varphi St)$ with $C = 1.92$, in order to retrieve the good trend with St. Note that this simple model, which was also used in Fox (2014) for the same test case, is just qualitative and valid for the range of conditions considered herein. A more refined analysis may be necessary for general situations.

8.2.1. *Decaying turbulence*

Concerning the values of other model constants, they are the same as in the stationary case, i.e. $C_{\epsilon 2} = C_{\epsilon 2p} = C_{\epsilon 2f}$, $\beta = \beta_f = \beta_p = 1$, $C_3 = C_{3f} = C_{3p} = 3.5$ and $C_0 = C_{0f} = C_{0p} = 1$. As $\mathcal{S}_f = 0$, the isotropic model equations for k_f, $k_{f@p}$, k_p and k_{fp} are solved directly:

$$\frac{\mathrm{d}k_f}{\mathrm{d}t} = \frac{2\varphi}{\tau_p}(k_{fp} - k_{f@p}) - \varepsilon_f, \tag{8.7a}$$

https://doi.org/10.1017/jfm.2018.895 Published online by Cambridge University Press

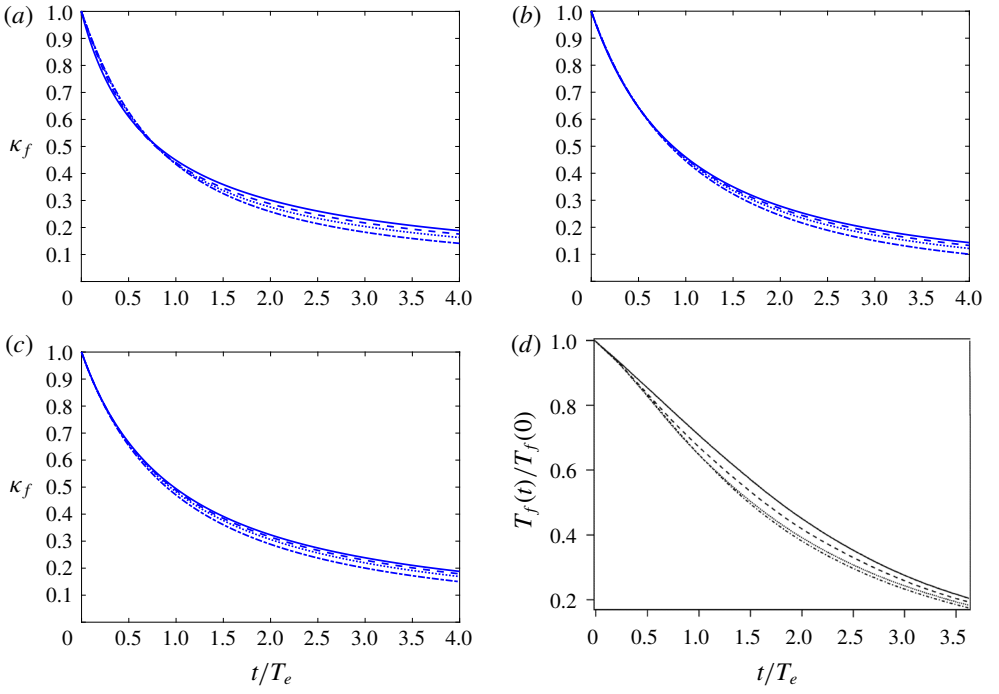


FIGURE 2. (Colour online) Fluid turbulent kinetic energy as a function of the non-dimensional time, t/T_e, in decaying fluid–particle turbulence: (*a*) complete particle model, (*b*) simplified particle model, (*c*) Fox (2014) Eulerian model and (*d*) DNS of Sundaram & Collins (1999). The curves correspond to four different Stokes numbers: $St = 0$, solid line; $St = 0.17$, dashed lines; $St = 0.35$, dotted lines; $St = 0.69$, dash-dotted lines. In panel (*d*) $T_f \propto k_f$.

$$\frac{\mathrm{d}k_{f@p}}{\mathrm{d}t} = \frac{2\varphi}{\tau_p}(k_{fp} - k_{f@p}) - \varepsilon_f, \tag{8.7b}$$

$$\frac{\mathrm{d}k_p}{\mathrm{d}t} = \frac{2}{\tau_p}(k_{fp} - k_p) - \varepsilon_p, \tag{8.7c}$$

$$\frac{\mathrm{d}k_{fp}}{\mathrm{d}t} = \frac{1}{\tau_p}[k_{f@p} + \varphi k_p - (1+\varphi)k_{fp}] - \left(\frac{1}{2} + \frac{3}{4}C_0\right)\left(\frac{\varepsilon_f}{k_f} + \frac{\varepsilon_p}{k_p}\right)k_{fp}, \tag{8.7d}$$

$$\frac{\mathrm{d}\varepsilon_f}{\mathrm{d}t} = -C_{\epsilon 2}\frac{\varepsilon_f^2}{k_f} + C_3\frac{\varphi}{\tau_p}\left(\frac{k_{fp}}{k_{f@p}}\varepsilon_p - \varepsilon_f\right), \tag{8.7e}$$

$$\frac{\mathrm{d}\varepsilon_p}{\mathrm{d}t} = -C_{\epsilon 2}\frac{\varepsilon_p^2}{k_p} + \frac{C_3}{\tau_p}\left(\frac{k_{fp}}{k_{f@p}}\varepsilon_f - \varepsilon_p\right). \tag{8.7f}$$

In the decaying turbulence test, initial conditions for the simulation are $k_f(0) = k_{f@p}(0) = k_p(0) = k_{fp}(0) = 1.314$, in accordance with the DNS by Sundaram & Collins (1999), and $\varepsilon_f(0) = \varepsilon_p(0) = 1.0112$. Moreover, the mass loading is set to $\varphi = 0.162$. Note that because $k_f(0) = k_{f@p}(0)$, the first two equations in system (8.7) will yield $k_f(t) = k_{f@p}(t)$ so that only k_f is required to model decaying turbulence for this case.

Figure 2(*a*) shows the time evolution of the fluid turbulent kinetic energy obtained with the particle models, for particle sets characterised by four different Stokes

https://doi.org/10.1017/jfm.2018.895 Published online by Cambridge University Press

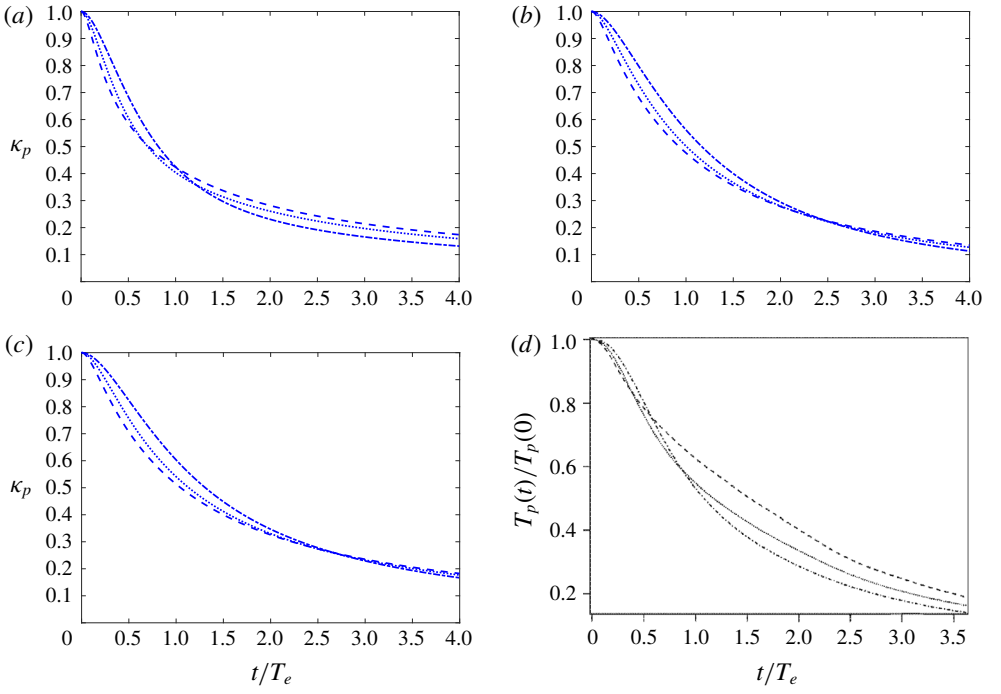


FIGURE 3. (Colour online) Particle-phase fluctuating energy as a function of the non-dimensional time, t/T_e, in decaying fluid–particle turbulence: (*a*) complete particle model, (*b*) simplified particle model, (*c*) Eulerian model of Fox (2014) and (*d*) DNS of Sundaram & Collins (1999). The curves correspond to the following Stokes numbers: $St = 0.17$, dashed lines; $St = 0.35$, dotted lines; $St = 0.69$, dash-dotted lines. In panel (*d*) $T_f \propto k_f$.

numbers, namely $St = \tau_p/T_e = 0$ (fluid tracers), $St = 0.17$, $St = 0.35$ and $St = 0.69$ (where $T_e = 1.7328$ is the initial eddy turnover time in DNS of Sundaram & Collins (1999)). Note that the case at $St = 0$ was obtained from the particle equations as the limit case for $\tau_p/T_L \ll 1$, as described in appendix A. Figure 2(*b–d*) shows the same quantities as in figure 2(*a*), obtained by the simplified version of the present model, the Eulerian model by Fox (2014) and the DNS by Sundaram & Collins (1999) respectively. The same comparisons for the particle-phase turbulent kinetic energy are reported in figure 3. It can be seen that the effect of the Stokes number on the decay of the turbulent kinetic energy of both the fluid and the particle phases is qualitatively well captured by the present stochastic model, in its complete version as well as in the simplified one, although the initial stages of the time evolution are quite different from the DNS results.

8.2.2. *Homogeneous-shear flow*

We consider now the case of a homogeneous-shear flow with $\mathcal{S}_f = 0.6$ as in Fox (2014), and solve the anisotropic model equations given in § 7. The mass loading is $\varphi = 0.162$ and the initial conditions $\varepsilon_f(0) = \varepsilon_p(0) = 0.25$. As in the previous decaying case, simulations have been carried out for the following four Stokes numbers: $St = 0, 0.17, 0.35, 0.69$. The values of the constants in our model are the same as in the previous case of homogeneous decaying turbulence with $C_{\epsilon 1f} = C_{\epsilon 1p} = 1.44$, which are

https://doi.org/10.1017/jfm.2018.895 Published online by Cambridge University Press

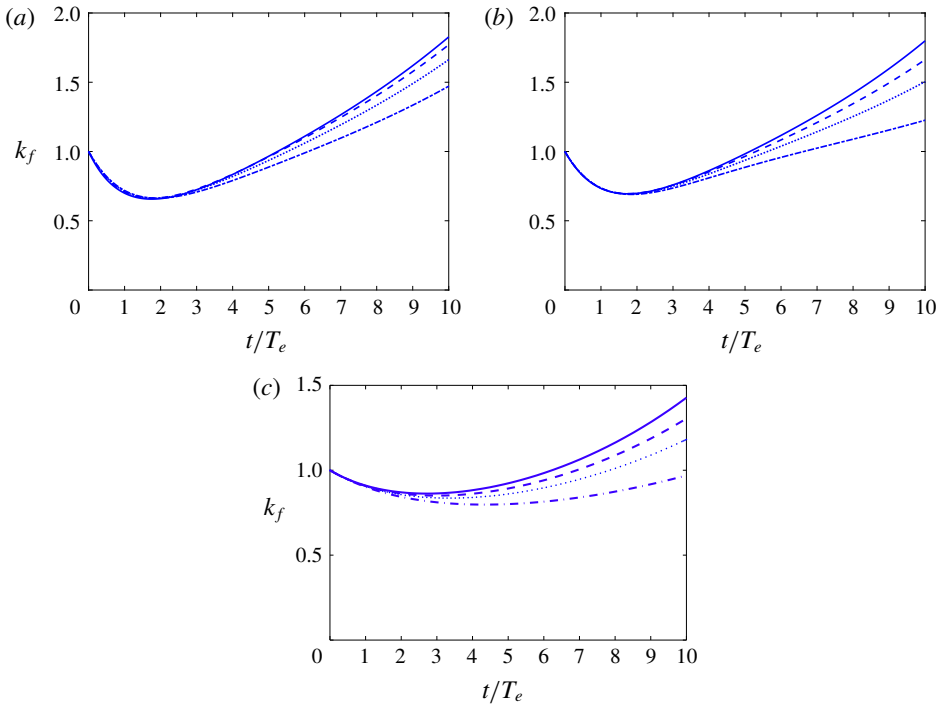


FIGURE 4. (Colour online) Homogeneous-shear flow. Fluid turbulent kinetic energy as a function of the non-dimensional time, t/T_e with (*a*) the complete stochastic model, (*b*) the simplified stochastic model and (*c*) the Eulerian model by Fox (2014). The curves correspond to four different Stokes numbers: $St = 0$, solid line; $St = 0.17$, dashed lines; $St = 0.35$, dotted lines; $St = 0.69$, dash-dotted lines.

standard values for single-phase turbulence models (Pope 2000). For the simplified model $C_{\epsilon 1f} = 1.2$. Figure 4 shows the time evolution of the fluid turbulent kinetic energy obtained with the particle model, both in its complete and simplified versions, with the same quantity obtained from the Eulerian model in Fox (2014). Comparison should also be made with the DNS data of Ahmed & Elghobashi (2000). For all the models, the time behaviour is qualitatively similar to that observed in DNS, with an initial decrease of the fluid turbulent kinetic energy followed by an increase. The value of the minima of k_f given by the complete model are closer to those obtained in DNS. Moreover, the effect of particle inertia on the time evolution of k_f is also correctly captured, i.e. the rate of increase of the fluid turbulent kinetic energy after the minimum is reduced as the inertia of the particles increases. The same effect is found also for the particle-phase fluctuating energy, κ_p, in agreement with Fox (2014), as can be seen in figure 5. No DNS data are available for this quantity.

8.3. *Cluster-induced turbulence*

To isolate the effect of turbulence generated by particles through two-way coupling, we consider a flow initially at rest laden with a random distribution of finite-size particles of diameter d_p subject to gravity oriented in the downward x_1 direction. The physical parameters are chosen to correspond to the Euler–Lagrange (EL) point-particle simulation of Capecelatro *et al.* (2015) as summarised in table 1.

https://doi.org/10.1017/jfm.2018.895 Published online by Cambridge University Press

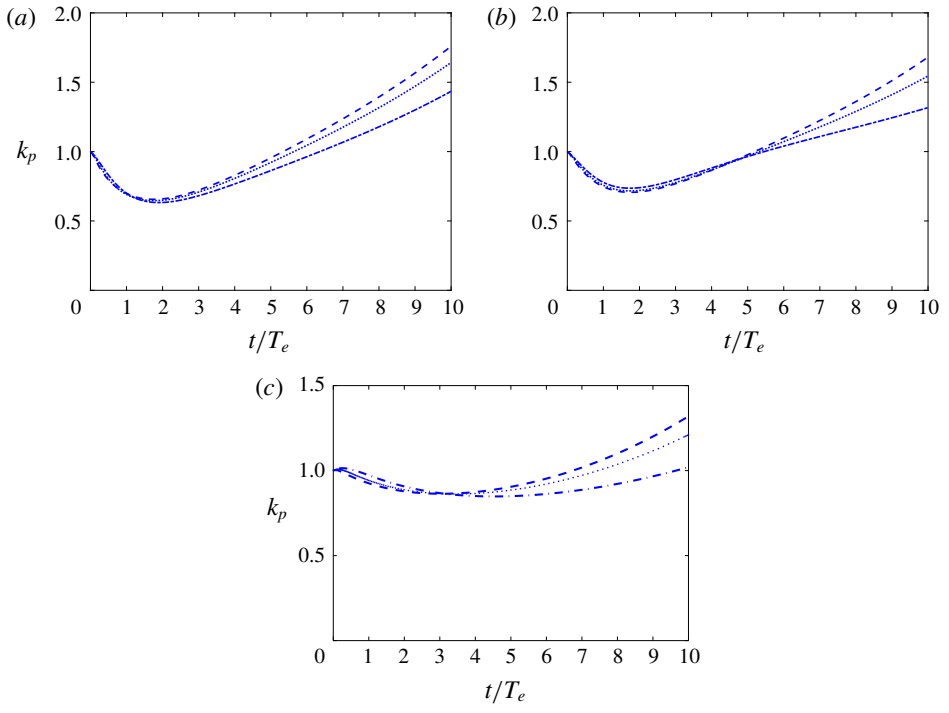


FIGURE 5. (Colour online) Homogeneous-shear flow. Particle-phase fluctuating energy as a function of the non-dimensional time, t/T_e with (*a*) complete particle model, (*b*) simplified particle model and (*c*) Eulerian model in Fox (2014). The curves correspond to the Stokes numbers: $St = 0.17$, dashed lines; $St = 0.35$, dotted lines; $St = 0.69$, dash-dotted lines.

The dimensionless two-phase parameters that characterise the flow include the particle-to-fluid density ratio $\rho_p/\rho_f = 1000$, the average particle-phase volume fraction $\langle\alpha_p\rangle = 0.01$ and the particle Reynolds numbers $Re_p = \tau_p g d_p/\nu_f = 1$ where $\tau_p = \rho_p d_p^2/(18\rho_f\nu_f)$ is the particle relaxation time, ν_f is the fluid-phase kinematic viscosity and g is the magnitude of the gravity vector. Combination of these non-dimensional numbers yields the mass loading $\varphi = \rho_p\langle\alpha_p\rangle/(\rho_f\langle\alpha_f\rangle) = 10.1$, where $\langle\alpha_f\rangle = 1 - \langle\alpha_p\rangle$ is the average fluid-phase volume fraction. Finally, $\mathcal{V} = g\tau_p$ is the settling velocity for a single particle.

The CIT case is statistically homogeneous in all directions with periodic boundary conditions; therefore, in the context of the present formalism, it reduces to a zero-dimensional description, with only the time dependence. Moreover, as in the previous considered cases, since the RA equations obtained from the stochastic ones are in closed form for a homogeneous configuration, we can limit ourselves to solving a system of coupled ordinary differential equations (ODEs), instead of carrying out a Lagrangian Monte Carlo simulation. The simulation is performed starting from an initial condition where both the particle and fluid phases are at rest and it is evolved in time up to the steady state. The fluid-phase pressure gradient is dynamically adjusted in order to keep the mean fluid velocity $\langle\boldsymbol{U}_f\rangle$ equal to zero. The model constants have been set in order to obtain a good prediction of the steady-state values for first-order moments. The values, so obtained, are reported in tables 2–3. A comment is in order concerning the values of C_{0f} and C_{3p}. These values are taken different from those used

https://doi.org/10.1017/jfm.2018.895 Published online by Cambridge University Press

	Physical parameters	
d_p	Particle diameter	0.09 mm
ρ_p	Particle density	1000 kg m^{-3}
ρ_f	Fluid density	1 kg m^{-3}
ν_f	Fluid kinematic viscosity	1.8×10^{-5} m^2 s^{-1}
g	Gravity magnitude	8 m s^{-2}
	Non-dimensional parameters	
e	Restitution coefficient	0.90
$\langle\alpha_p\rangle$	Mean particle volume fraction	0.01
φ	Mean mass loading	10.1
Re_p	Particle Reynolds number	1
	Dimensional parameters	
τ_p	Drag time	0.025 s
$\mathcal{V}$	Settling velocity	0.20 m s^{-1}

TABLE 1. Fluid–particle parameters used in CIT simulations (Capecelatro *et al.* 2015).

C_{0f}	C_{0p}	$C_{\epsilon 2}$	C_{3f}	C_{3p}	C_4	f_s	β_f	C_c
3.5	0.18	1.92	3.5	7.0	6.81	0.4	1	1

TABLE 2. Values of the model constants used in CIT simulations for the complete model.

C_{0f}	$C_{\epsilon 2}$	C_{3f}	C_4	β_f
0.8	6	0.02	0.1	0.75

TABLE 3. Values of the model constants used in CIT simulations for the simplified model.

in the isotropic cases previously analysed. The results obtained in the CIT case with the previous values are in reasonable agreement with the full numerical simulation, but show some discrepancy which has been eliminated using the values proposed in table 2. In fact, C_{3p} has an insignificant effect on the asymptotic results, but the present higher value smooths the transient dynamics. In contrast, the value of C_{0f} turns out to be key to get the correct level of turbulent kinetic energy.

The steady-state solution of first-order moments equations yields $\langle U_{s,1} - U_{p,1}\rangle = \mathcal{V}$, which agrees with the EL simulations of Capecelatro *et al.* (2015), and

$$\langle U_{s,1}\rangle = -\langle\alpha_p\rangle(1+\varphi)\frac{T^*_{L,1}}{\tau_p}\mathcal{V}, \tag{8.8}$$

where, using the definition in § 4.1,

$$\frac{T^*_{L,1}}{\tau_p} = \left[\left(\frac{1}{2}+\frac{3}{4}C_{0f}\right)^2\left(1+\frac{3\beta^2\mathcal{V}^2}{2k_f}\right)\right]^{-1/2}\frac{1}{St_f} \tag{8.9}$$

and $St_f = (\tau_p\varepsilon_f/k_f)$; $\beta = T_{Lf}/T_{Ef}$ is set equal to 0.8. In fully developed CIT, the turbulence is generated by the clusters and the resulting Stokes number is nearly constant (Capecelatro *et al.* 2016*b*). The complete model therefore predicts that the steady-state value of $\langle U_{s,1}\rangle/\mathcal{V}$ depends on the particle volume fraction, the mass

https://doi.org/10.1017/jfm.2018.895 Published online by Cambridge University Press

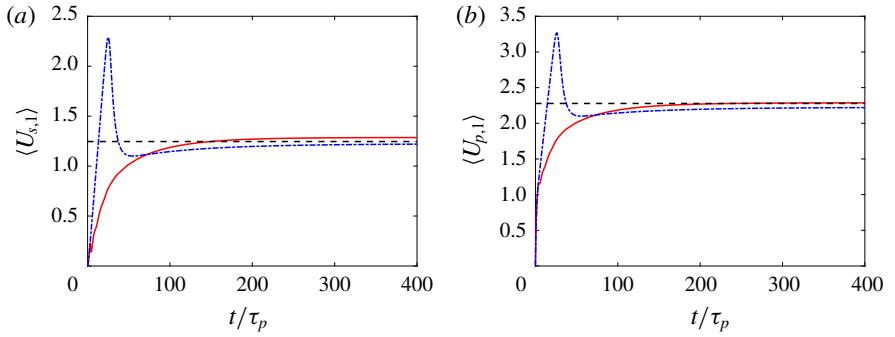


FIGURE 6. (Colour online) Time evolution of the vertical mean fluid velocity seen by the particles (*a*) and of the vertical mean particle velocity (*b*) from the complete (red line) and from the simplified (blue dot-dashed line) stochastic model. The horizontal black dashed line represents the steady-state mean velocity from the DNS of Capecelatro *et al.* (2015).

loading and the dimensionless fluid-phase turbulent kinetic energy $2k_f/\mathcal{V}^2$. The prediction of $\langle \boldsymbol{U}_s \rangle$ is perhaps the most important contribution of the Lagrangian pdf model for CIT because information on the fluid seen by the particles is not available in most multiphase turbulence models for fluid–particle flows (see e.g. Fox 2014, for details).

The second-order moments have two independent, non-zero components, i.e. the vertical (1, 1) and horizontal (2, 2). For the fluid phase, these are found by solving (7.27). In CIT, the fluid-phase Reynolds stresses are anisotropic because of the mean velocities appearing in $\mathcal{P}_{f,11}$. In general, redistribution is weak so that $\langle u_{f,2}^2 \rangle \ll \langle u_{f,1}^2 \rangle$. In CIT, the anisotropy of the particle-phase pressure tensor arises due to the source terms $\varepsilon_{p,11}$, $\varepsilon_{p,22}$, whose anisotropy is controlled by f_s. For example, if $f_s = 1$ and collisions are negligible, the particle-phase pressure tensor and Reynolds stresses will have the same anisotropy. The value of the free parameter C_c in the collision term, on the other hand, will control the anisotropy of the particle-phase pressure tensor. For the particle phase, the Reynolds stresses are found by solving (7.6). The anisotropy of the particle-phase Reynolds stresses arises due to the production terms, i.e. due to the anisotropy of $\langle u_{s,i} u_{p,j} \rangle$. The latter are found by solving (6.12). Likewise, the Reynolds stresses for the fluid seen by the particles are found from (7.10). As seen for the fluid phase, the anisotropy of fluid seen is mainly due to the production terms, but is also due to the directional dependence of $T^*_{L,i}$. The dissipation rates ε_p and ε_f are found by solving (7.16) and (7.30) with the mean-shear-production terms set to zero.

Figures 6–8 show the time evolution of some mean velocities and second-order moments of both the fluid and particle phases, obtained with the complete and simplified models. It can be seen that all the quantities, after a transient of about 80–$100\tau_p$ due to the non-trivial coupling between particles and fluid, tend to a steady value. The dashed horizontal line in the figures is the steady-state value obtained in the EL simulation by Capecelatro *et al.* (2015). It can be seen that the mean velocities (figure 6) are well captured by both the complete and simplified models. As anticipated, an important feature of the Lagrangian pdf models is to provide a prediction of the fluid velocity seen by the particles, as compared to Eulerian pdf models in which it must be *a priori* specified. As for the second-order moments (figures 7 and 8), the complete model still gives a good agreement with

https://doi.org/10.1017/jfm.2018.895 Published online by Cambridge University Press

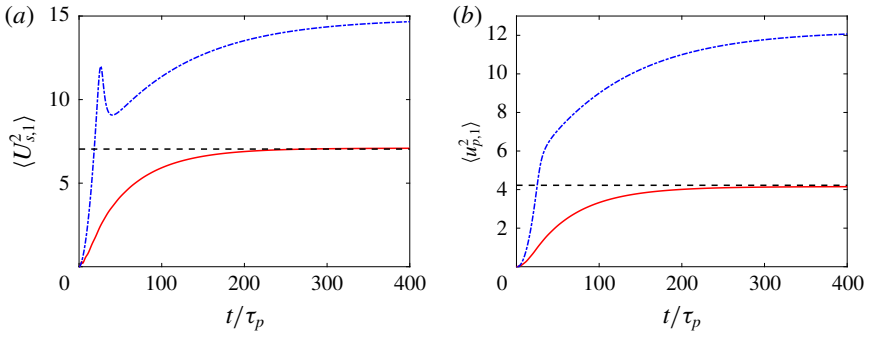


FIGURE 7. (Colour online) Time evolution of second-order moments of the vertical mean fluid velocity seen by the particles (*a*) and of the vertical mean particle velocity (*b*) from the complete (red line) and from the simplified (blue dot-dashed line) stochastic model. The horizontal black dashed line represents the steady-state mean velocity from the DNS of Capecelatro *et al.* (2015).

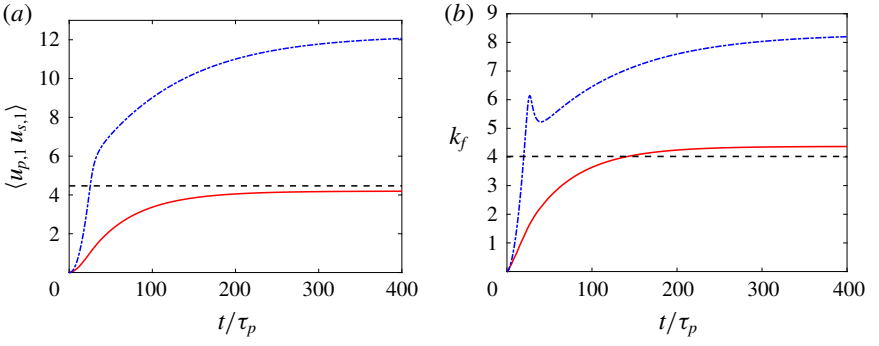


FIGURE 8. (Colour online) Time evolution of $\langle u_{p,1} u_{s,1} \rangle$ (*a*) and of k_f (*b*) from the complete (red line) and from the simplified (blue dot-dashed line) stochastic model. The horizontal black dashed line represents the steady-state mean velocity from the DNS of Capecelatro *et al.* (2015).

	$2k_f/\mathcal{V}^2$	$\langle u_{f,1}^2 \rangle/(2k_f)$	$\langle u_{f,2}^2 \rangle/(2k_f)$
EL simulation	8.04	0.82	0.09
Complete model	8.74	0.93	0.04
Simplified model	16.60	0.98	0.01

TABLE 4. Steady-state values of fluid-phase velocity statistics. EL simulation data are taken from Capecelatro *et al.* (2015).

EL simulations for both the fluid and particle phases, while the simplified version significantly overestimates the steady-state values.

Tables 4–6, in which the steady-state values of particle and fluid statistics are reported, confirm the previous observations. Table 5 also shows the repartition of the particle turbulent kinetic energy, κ_p, into the coherent part, k_p, and granular temperature, Θ_p. For the simplified model, by definition, $\Theta_p = 0$ and $\kappa_p = k_p$.

https://doi.org/10.1017/jfm.2018.895 Published online by Cambridge University Press

	$\langle U_{p,1}\rangle/\mathcal{V}$		
EL simulation	−2.28		
Complete model	−2.28		
Simplified model	−2.22		
	$2\kappa_p/\mathcal{V}^2$	$\langle v_{p,1}^2\rangle/(2\kappa_p)$	$\langle v_{p,2}^2\rangle/(2\kappa_p)$
EL simulation	5.41	0.78	0.11
Complete model	5.13	0.81	0.09
Simplified model	12.71	0.96	0.02
	k_p/κ_p	$\langle u_{p,1}^2\rangle/(2k_p)$	$\langle u_{p,2}^2\rangle/(2k_p)$
EL simulation	0.89	0.81	0.09
Complete model	0.99	0.81	0.09
	$3\langle\Theta_p\rangle/(2\kappa_p)$	$\langle P_{11}\rangle/(3\langle\Theta_p\rangle)$	$\langle P_{22}\rangle/(3\langle\Theta_p\rangle)$
EL simulation	0.11	0.51	0.25
Complete model	0.01	0.49	0.25

TABLE 5. CIT: steady-state values of particle-phase velocity statistics. EL simulation data are taken from Capecelatro *et al.* (2015).

	$\langle U_{s,1}\rangle/\mathcal{V}$		
EL simulation	−1.25		
Complete model	−1.28		
Simplified model	−1.22		
	$2k_{f@p}/\mathcal{V}^2$	$\langle u_{s,1}^2\rangle/(2k_{f@p})$	$\langle u_{s,2}^2\rangle/(2k_{f@p})$
EL simulation	8.32	0.85	0.07
Complete model	8.06	0.88	0.06
Simplified model	15.36	0.96	0.02
	$2k_{fp}/\mathcal{V}^2$	$\langle u_{s,1}u_{p,1}\rangle/(2k_{fp})$	$\langle u_{s,2}u_{p,2}\rangle/(2k_{fp})$
EL simulation	5.45	0.82	0.09
Complete model	5.13	0.82	0.09
Simplified model	12.71	0.96	0.02

TABLE 6. CIT: steady-state values of fluid-phase turbulence statistics seen by particles. EL simulation data are taken from Capecelatro *et al.* (2015).

The complete model also underestimates the granular temperature, most likely due to underestimating the value of ε_p through the choice of C_{3p}. Nonetheless, the decomposition of the particle turbulent kinetic energy appears to be essential to well predict second-order statistics, as done by the complete model in contrast to the simplified one. The complete model also well reproduces the fact that for all the quantities, except for the uncorrelated part of the particle velocity, turbulence fluctuations in the vertical direction are much higher than those in the horizontal directions. The complete model is able to correctly reproduce the anisotropy of the second-order tensors while the simplified model only gives a qualitative agreement.

https://doi.org/10.1017/jfm.2018.895 Published online by Cambridge University Press

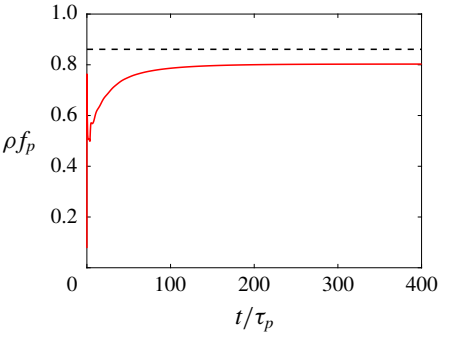


FIGURE 9. (Colour online) Time evolution of $\rho_{fp} = k_{fp}/(k_{f@p}k_p)^{1/2}$ from the complete stochastic model. The horizontal black dashed line represents the steady-state mean value from the DNS of Capecelatro *et al.* (2015).

Finally, figure 9 shows the time evolution of the correlation coefficient

$$\rho_{fp} = \frac{k_{fp}}{\sqrt{k_{f@p}k_p}}, \tag{8.10}$$

which proves the importance of having a stochastic model that predicts k_{fp}, leading to a correlation coefficient ρ_{fp} that can vary in time, instead of setting it to a constant value. Moreover, we can then use ρ_{fp} in the dissipation–exchange terms in (6.9) and (6.10). For example, similar to the model proposed by Fox (2014), $k_{fp}\varepsilon_f/k_{f@p}$ and $k_{fp}\varepsilon_p/k_{f@p}$ in (6.9) and (6.10), respectively, could be replaced with $\rho_{fp}\sqrt{\varepsilon_p\varepsilon_f}$, which may help to increase the value of ε_p when applied to CIT.

9. Discussion and conclusions

The main objective of this work was to develop a novel pdf modelling approach for particle-laden turbulent flows including in a statistical sense particle–particle collisions. The approach is based on the development of a modelled equation for the one-particle Lagrangian pdf. As for the single-phase turbulent pdf approach (Pope 2000; Fox 2003), the corresponding Reynolds-averaged moment equations are taken as a useful guideline for the construction of a sound model. In the present case, the recent Reynolds-averaged framework developed by Fox (2014) and validated in Capecelatro *et al.* (2016*b*) has been taken as reference. One of the most original points of the present approach consists in developing a Lagrangian pdf model based upon the decomposition of the velocity into two separate particle-phase velocity variables ($\boldsymbol{U}_p$ and $\delta\boldsymbol{v}_p$), which are statistically uncorrelated. This decomposition has been found to be key in the correct reproduction of moderately dense particle flows and has been never used before in the framework of Lagrangian pdf modelling, where only the total particle velocity is available.

The new framework put forward is very general, but a precise model has to be proposed to make actual simulations. From a technical point of view, we have proposed a new stochastic model, which represents the joint state variables ($\boldsymbol{x}_p$, $\boldsymbol{V}_p$, $\delta\boldsymbol{v}_p$, $\boldsymbol{U}_s$) as a diffusion process, or informally a Langevin equation, that is, the corresponding joint pdf is given by a Fokker–Planck equation. The model has been built phenomenologically, and the unclosed terms in the exact Lagrangian

https://doi.org/10.1017/jfm.2018.895 Published online by Cambridge University Press

equations have been replaced by return-to-equilibrium and fluctuating terms, following fluctuation–dissipation arguments (Marconi *et al.* 2008). To highlight the role of the decomposition of the velocity, we have also developed a simplified model that takes into account the two-way coupling between the phases but does not consider the presence of an uncorrelated part of the velocity. This model bears some similarity to a previous proposition (Minier & Peirano 2001; Peirano *et al.* 2006), but in fact even this model is new since it differs in the closure of the drift and diffusion coefficients. In particular, it has been built to describe the presence of a drift velocity even in homogeneous cases. The Reynolds-averaged equations derived from the complete pdf model are shown to be consistent with the ones obtained in the Eulerian framework (Fox 2014). On the other hand, and this is one of the significant advantages of Lagrangian pdf approaches (Pope 2000; Minier & Peirano 2001), the level of content of the present model is more detailed, notably the fluid velocity seen by the particles $\boldsymbol{U}_s$ is included and therefore all the related one-point moments can be computed. When the mean mass loading is non-negligible, the dynamics of the fluid velocity seen by the particles is strongly affected by coupling with the particle phase. The Lagrangian pdf model thus provides a closure for the moments of $\boldsymbol{U}_s$, which need a closure in the Eulerian framework. It is expected that the present model has the same range of validity as the corresponding Eulerian one, namely it should be valid for moderate mean mass loadings where volume fraction is only a few per cent $\alpha_p \leqslant 0.05$. For higher mass loading, new terms should be added taking into account rheological effects. This is a challenging and interesting perspective.

Once the pdf formalism and the Lagrangian pdf model were defined, we validated it using the same test cases employed to validate a recently developed Eulerian model (Fox 2014; Capecelatro *et al.* 2015). In particular, the Lagrangian pdf model is applied to statistically homogeneous flows of increasing difficulty, namely, (i) particle-laden homogeneous isotropic turbulence (Février *et al.* 2005; Sundaram & Collins 1999), (ii) homogeneous sheared turbulence (Elghobashi 1994) and (iii) CIT (Capecelatro *et al.* 2015). In the first two cases, the mean fluid- and particle-phase velocities are null, and hence the production of fluid-phase turbulence by fluid drag is absent. These cases are useful for validating the coupling terms in the Lagrangian pdf model for the exchange of turbulent kinetic energy between the two phases, and their dependence on the mass loading. In contrast, case (iii) provides a difficult and physically more interesting validation test of the model for $\langle \boldsymbol{U}_s \rangle$. Indeed it determines the mean slip velocity between the two phases (see (6.3)), and of the exchange/dissipation models, which determine the relative contributions of correlated k_p and uncorrelated Θ_p turbulent kinetic energy. Interestingly, the steady-state model for $\langle \boldsymbol{U}_s \rangle$ given in (8.8) is relatively simple (compare, for example, the correlation used in Capecelatro *et al.* 2016*b*), with the Lagrangian time scale $T^*_{L,1}$ playing a prominent role. The complete and simplified models are both qualitatively in agreement with DNS and experiments in the homogeneous isotropic and shear cases, although the simplified model cannot predict the quantities related to the uncorrelated part of the velocity. Instead, important differences are encountered for the CIT case. While the complete pdf model gives satisfactory results for all observables, the simplified model is able to provide good predictions for the first moments but strongly overestimates the energy. This result is important, since it demonstrates that the decomposition of the particle velocity into correlated and uncorrelated parts is necessary to correctly represent the dynamics of moderately dense flows. From a physical point of view, it is interesting to note, however, that even though the agreement is only qualitative, the simple two-way coupling, without collisions, is able to induce CIT.

https://doi.org/10.1017/jfm.2018.895 Published online by Cambridge University Press

To conclude, in this work we have developed a general approach, in which we have proposed a specific model validated in some relevant test cases. To assess and improve the model, it would be interesting, in future work, to investigate CIT over a wide range of $\langle\alpha_p\rangle$ and φ values to determine whether the parameters in the model for $T^*_{L,1}$ should depend on these quantities. In fact, it would be useful to develop a model for the fluid pressure gradient seen by particles directly from DNS. More generally, the complete pdf model should be tested for inhomogeneous particle-laden flows wherein the spatial transport terms play an important role. For example, the particle-laden channel flows of Capecelatro *et al.* (2016*a*), Capecelatro, Desjardins & Fox (2018) would be challenging test cases. In particular, for channel flows the correlated and uncorrelated particle velocity components generate separate spatial fluxes for all statistics. From the RA model developed in Capecelatro *et al.* (2016*b*), it is known that, depending on the Stokes number, one or the other of these fluxes may be dominant. As a result, the wall-normal distribution of $\langle\alpha_p\rangle$, as well as other statistics, is very sensitive to how the spatial fluxes are modelled. In any case, as shown in this work, it can be expected that by including a stochastic model for $\boldsymbol{U}_s$ the resulting models for the spatial fluxes will provide more robust closures for inhomogeneous turbulent particle-laden flows.

Acknowledgements

We thank Dr A. Vichansky for his remarks during the revision process. R.O.F. was partially supported by grants from the US National Science Foundation (CBET-1437865 and ACI-1440443).

Appendix A. Exact Reynolds-averaged equations

A.1. *Particle phase*

We show here the RA form of the Lagrangian pdf transport equations (2.9). It is worth noting that they correspond exactly to the RA transport equations obtained in Capecelatro *et al.* (2015) from the corresponding hydrodynamics ones. From the equation for $\widetilde{\boldsymbol{V}}_p$ (2.9), applying an RA (ensemble-averaging over a large number of fluid realisations), the exact RA equations can be retrieved for the particle mean velocity $\langle\boldsymbol{V}_p\rangle = \langle\widetilde{\boldsymbol{V}}_p\rangle$:

$$\frac{\partial\langle\alpha_p\rangle\langle\widetilde{\boldsymbol{V}}_p\rangle}{\partial t} + \boldsymbol{\nabla}\cdot\langle\alpha_p\rangle(\langle\widetilde{\boldsymbol{V}}_p\rangle\otimes\langle\widetilde{\boldsymbol{V}}_p\rangle + \langle\mathcal{P}\rangle) = \langle\alpha_p\rangle\left(\left\langle\frac{\widetilde{\boldsymbol{U}}_f - \widetilde{\boldsymbol{V}}_p}{\tau_p}\right\rangle + \boldsymbol{g}\right), \tag{A 1}$$

where $\langle\mathcal{P}\rangle = \langle\boldsymbol{P}\rangle + \langle\widetilde{\boldsymbol{v}}_p\otimes\widetilde{\boldsymbol{v}}_p\rangle$. The Reynolds stresses of the correlated part $\langle\widetilde{\boldsymbol{v}}_p\otimes\widetilde{\boldsymbol{v}}_p\rangle$ can be obtained analogously, and it gives the following Eulerian transport equation:

$$\begin{aligned}&\frac{\partial\langle\alpha_p\rangle\langle\widetilde{\boldsymbol{v}}_p\otimes\widetilde{\boldsymbol{v}}_p\rangle}{\partial t} + \boldsymbol{\nabla}\cdot\langle\alpha_p\rangle(\langle\widetilde{\boldsymbol{V}}_p\rangle\otimes\langle\widetilde{\boldsymbol{v}}_p\otimes\widetilde{\boldsymbol{v}}_p\rangle) + \boldsymbol{\nabla}\cdot\langle\alpha_p\rangle\langle\widetilde{\boldsymbol{v}}_p\otimes\widetilde{\boldsymbol{v}}_p\otimes\widetilde{\boldsymbol{v}}_p\rangle\\ &\quad= -\langle\alpha_p\rangle(\langle\widetilde{\boldsymbol{v}}_p\otimes\widetilde{\boldsymbol{v}}_p\rangle\cdot\boldsymbol{\nabla}\langle\widetilde{\boldsymbol{V}}_p\rangle)^\dagger - \langle\alpha_p\rangle\langle\widetilde{\boldsymbol{v}}_p\otimes\boldsymbol{\nabla}\cdot(\delta\widetilde{\boldsymbol{V}_p\otimes\delta\boldsymbol{V}_p})\rangle^\dagger\\ &\qquad+\langle\alpha_p\rangle\frac{(\langle\widetilde{\boldsymbol{u}}_f\otimes\widetilde{\boldsymbol{v}}_p\rangle - \langle\widetilde{\boldsymbol{v}}_p\otimes\widetilde{\boldsymbol{v}}_p\rangle)^\dagger}{\tau_p}.\end{aligned} \tag{A 2}$$

Finally, applying first the coarse-graining operator and then the RA one to (2.8), we

https://doi.org/10.1017/jfm.2018.895 Published online by Cambridge University Press

get the equation for the particle-phase pressure tensor:

$$\frac{\partial \langle\alpha_p\rangle\langle \boldsymbol{P}\rangle}{\partial t} + \boldsymbol{\nabla}\cdot\langle\alpha_p\rangle\left(\langle\widetilde{\boldsymbol{V}}_p\rangle\otimes\langle\boldsymbol{P}\rangle + \langle\delta\widetilde{\boldsymbol{V}_p\otimes\delta\boldsymbol{V}}_p\otimes\delta\boldsymbol{V}_p\rangle + \langle\delta\widetilde{\boldsymbol{V}_p\otimes\delta\boldsymbol{V}}_p\otimes\widetilde{\boldsymbol{v}}_p\rangle\right)$$
$$= -2\langle\alpha_p\rangle\frac{\langle\boldsymbol{P}\rangle}{\tau_p} - \langle\alpha_p\rangle(\langle\boldsymbol{P}\rangle\cdot\boldsymbol{\nabla}\langle\widetilde{\boldsymbol{V}}_p\rangle)^{\dagger} - \langle\alpha_p\rangle\langle\boldsymbol{P}\cdot\boldsymbol{\nabla}\widetilde{\boldsymbol{v}}_p\rangle^{\dagger}. \tag{A 3}$$

A.2. *Fluid phase*

Taking the RA of the hydrodynamic fluid-phase equations (see Capecelatro *et al.* 2015) yields the RA fluid-phase transport equation. It gives for the volume fraction:

$$\frac{\partial\langle\alpha_f\rangle}{\partial t} + \boldsymbol{\nabla}\cdot\langle\alpha_f\rangle\langle\boldsymbol{U}_f\rangle_f = 0. \tag{A 4}$$

For the fluid velocity:

$$\frac{\partial\langle\alpha_f\rangle\langle\boldsymbol{U}_f\rangle_f}{\partial t} + \boldsymbol{\nabla}\cdot\langle\alpha_f\rangle(\langle\boldsymbol{U}_f\rangle_f\otimes\langle\boldsymbol{U}_f\rangle_f + \langle\boldsymbol{u}_f\otimes\boldsymbol{u}_f\rangle_f)$$
$$= -\frac{\langle\alpha_f\rangle}{\rho_f}\boldsymbol{\nabla}\langle p_f\rangle + \frac{\langle\alpha_f\rangle}{\rho_f}\boldsymbol{\nabla}\cdot\langle\boldsymbol{\sigma}_f\rangle - \langle\alpha_f\rangle\varphi\left\langle\frac{\boldsymbol{U}_f-\boldsymbol{U}_p}{\tau_p}\right\rangle_p + \langle\alpha_f\rangle\boldsymbol{g}, \tag{A 5}$$

where

$$\varphi = \frac{\rho_p\langle\alpha_p\rangle}{\rho_f\langle\alpha_f\rangle} \tag{A 6}$$

is the mean mass loading, $\langle\boldsymbol{\sigma}_f\rangle$ is the viscous stress tensor and $\langle\boldsymbol{u}_f\otimes\boldsymbol{u}_f\rangle_f$ is the fluid-phase Reynolds-stress tensor.

And for the Reynolds-stress tensor we find

$$\frac{\partial\langle\alpha_f\rangle\langle\boldsymbol{u}_f\otimes\boldsymbol{u}_f\rangle_f}{\partial t} + \boldsymbol{\nabla}\cdot\langle\alpha_f\rangle(\langle\boldsymbol{U}_f\rangle_f\otimes\langle\boldsymbol{u}_f\otimes\boldsymbol{u}_f\rangle_f + \langle\boldsymbol{u}_f\otimes\boldsymbol{u}_f\otimes\boldsymbol{u}_f\rangle_f)$$
$$= -\langle\alpha_f\rangle(\langle\boldsymbol{u}_f\otimes\boldsymbol{u}_f\rangle_f\cdot\boldsymbol{\nabla}\langle\boldsymbol{U}_f\rangle_f)^{\dagger} + \frac{\langle\alpha_f\rangle}{\rho_f}(\boldsymbol{\nabla}\cdot\langle\boldsymbol{\sigma}_f\otimes\boldsymbol{u}_f\rangle - \boldsymbol{\nabla}\langle p_f\boldsymbol{u}_f\rangle)^{\dagger}$$
$$- \frac{\langle\alpha_f\rangle}{\rho_f}(\langle\boldsymbol{\sigma}_f\cdot\boldsymbol{\nabla}\boldsymbol{u}_f\rangle - \langle p_f\boldsymbol{\nabla}\boldsymbol{u}_f\rangle)^{\dagger}$$
$$+ \frac{\langle\alpha_f\rangle\varphi}{\tau_p}[\langle\boldsymbol{u}_f\otimes\boldsymbol{u}_p\rangle_p - \langle\boldsymbol{u}_f\otimes\boldsymbol{u}_f\rangle_p + \langle\boldsymbol{u}_f\rangle_p\otimes(\langle\boldsymbol{U}_p\rangle_p - \langle\boldsymbol{U}_f\rangle_f)]^{\dagger}. \tag{A 7}$$

The fluid-phase variables that are averaged with respect to the particle phase, i.e. $\langle\boldsymbol{u}_f\rangle_p$, appear due to fluid–particle coupling (e.g. due to clusters).

Appendix B. Simulation of a Gaussian vector: the Cholesky decomposition

Let $\boldsymbol{X} = (X_1, \ldots, X_d)$ be a Gaussian vector defined by a zero mean and a covariance matrix $C_{ij} = \langle X_i X_j\rangle$. For all positive symmetric matrices (such as C_{ij}), there exists a (lower or upper) triangular matrix P_{ij} which satisfies

$$\boldsymbol{C} = \boldsymbol{P}\boldsymbol{P}^t \Longrightarrow C_{ij} = \sum_{k=1}^{d} P_{ik}P_{jk}. \tag{B 1}$$

https://doi.org/10.1017/jfm.2018.895 Published online by Cambridge University Press

$\boldsymbol{P}$ is given by the Cholesky algorithm (here for the lower triangular matrix):

$$\left.\begin{aligned} P_{i1} &= \frac{C_{i1}}{\sqrt{C_{11}}}, \quad 1 \leqslant i \leqslant d, \\ P_{ii} &= \left(C_{ii} - \sum_{j=1}^{i-1} P_{ij} \right)^{1/2}, \quad 1 < i \leqslant d, \\ P_{ij} &= \frac{1}{P_{jj}} \left(C_{ij} - \sum_{k=1}^{j-1} P_{ik} P_{jk} \right), \quad 1 < j < i \leqslant d, \\ P_{ij} &= 0, \quad i < j \leqslant d. \end{aligned}\right\} \tag{B 2}$$

Let $\boldsymbol{G} = (G_1, \ldots, G_d)$ be a vector composed of independent $\mathcal{N}(0, 1)$ Gaussian random variables, then it can be shown that the vector $\boldsymbol{Y} = \boldsymbol{P}\boldsymbol{G}$ is a Gaussian vector of zero mean and whose covariance matrix is $\boldsymbol{C} = \boldsymbol{P}\boldsymbol{P}^t$. Therefore, $\boldsymbol{X}$ and $\boldsymbol{Y}$ are identical, that is,

$$\boldsymbol{X} = \boldsymbol{P}\boldsymbol{G} \Longrightarrow X_i = \sum_{k=1}^{d} P_{ik} G_k. \tag{B 3}$$

Appendix C. Fokker–Planck equation

The state vector of the Lagrangian description, given by $\boldsymbol{Z} = (\boldsymbol{x}_p, \boldsymbol{U}_p, \boldsymbol{\delta v}_p, \boldsymbol{U}_s)$, is associated with a single particle, while $\langle \boldsymbol{Z} \rangle$ stands for $\langle \boldsymbol{Z} \rangle [\boldsymbol{x}^{(k)}]$. The particle system is thus represented by this set of Lagrangian pdf equations, where the particle state variables are modelled through a Langevin equation, or to be more rigorous, as a diffusion process. This set of Lagrangian pdf equations for the trajectories of the sample particles corresponds, from the pdf point of view, to the following Fokker–Planck (FP) equation for the Eulerian mass density function (mdf) (Pope 1985; Minier & Peirano 2001; Fox 2003):

$$\begin{aligned} &\frac{\partial F_p^E}{\partial t} + U_{p,i} \frac{\partial F_p^E}{\partial x_i} + \delta \mathrm{v}_{p,i} \frac{\partial F_p^E}{\partial x_i} = -\frac{\partial}{\partial U_{p,i}} \left(\left[\frac{(U_{s,i} - U_{p,i})}{\tau_p} \right.\right. \\ &\quad \left.\left. - \frac{1}{\langle \alpha_p \rangle \rho_p} \frac{\partial \langle \alpha_p \rangle \rho_p \langle P_{ij} \rangle}{\partial x_j} + \delta \mathrm{v}_{p,j} \frac{\partial \langle U_{p,i} \rangle}{\partial x_j} - \frac{1}{T_{Lp}} (U_{p,i} - \langle U_{p,i} \rangle) + g_i \right] F_p^E \right) \\ &\quad + \frac{1}{2} C_p \varepsilon_p \delta_{ij} \frac{\partial^2 F_p^E}{\partial U_{p,i} \partial U_{p,j}} - \frac{\partial}{\partial \delta \mathrm{v}_{p,i}} \left(\left[-\frac{\delta \mathrm{v}_{p,i}}{\tau_p} \right.\right. \\ &\quad \left.\left. + \frac{1}{\langle \alpha_p \rangle \rho_p} \frac{\partial \langle \alpha_p \rangle \rho_p \langle P_{ij} \rangle}{\partial x_j} - \delta \mathrm{v}_{p,j} \frac{\partial \langle U_{p,i} \rangle}{\partial x_j} - \frac{(1+e)(3-e)}{4\tau_c} \delta \mathrm{v}_{p,i} \right] F_p^E \right) \\ &\quad + \frac{1}{2} \left[(B_\delta B_\delta^{\mathrm{T}})_{ij} + \frac{1}{2\tau_c} (1+e)^2 \langle \Theta_p \rangle \delta_{ij} \right] \frac{\partial^2 F_p^E}{\partial \delta \mathrm{v}_{p,i} \partial \delta \mathrm{v}_{p,j}} \\ &\quad + \left[\frac{\langle \alpha_f \rangle}{\rho_f} \frac{\partial \langle p_f \rangle}{\partial x_i} - (\langle U_{p,j} \rangle - \langle U_{f,j} \rangle) \frac{\partial \langle U_{f,i} \rangle}{\partial x_j} - g_i \right] \frac{\partial F_p^E}{\partial U_{s,i}} \\ &\quad - \frac{\partial}{\partial U_{s,i}} \left[\left(G_{ij} (U_{s,j} - \langle U_{f,j} \rangle) - \varphi \frac{(U_{s,i} - U_{p,i})}{\tau_p} \right) F_p^E \right] + \frac{1}{2} B_{s,ii}^2 \frac{\partial^2 F_p^E}{\partial U_{s,i} \partial U_{s,i}}, \end{aligned} \tag{C 1}$$

where $B_{s,ii}$ is the diffusion matrix given by (4.20), and it is not given here explicitly for the sake of clarity. $F_p^E(t, \boldsymbol{x}; \boldsymbol{U}_p, \boldsymbol{\delta v}_p, \boldsymbol{U}_s)$ is the probable mass of discrete particles in an element in the phase space of volume $\mathrm{d}\boldsymbol{U}_p\, \mathrm{d}\boldsymbol{\delta v}_p\, \mathrm{d}\boldsymbol{U}_s$ at a position $\boldsymbol{x}$.

https://doi.org/10.1017/jfm.2018.895 Published online by Cambridge University Press

Appendix D. Fluid–particle limit

The limit behaviour of the equations is only shown in homogeneous isotropic conditions for the sake of simplicity. In the limit case of tracer particles, i.e. $\tau_p \to 0$, we know from the equations for the stochastic model that $U_p \to U_s$ and $U_s \to U_f$, but we do not know if the model equation for U_s is exactly the same as U_p. At the same time we have that the particle-phase uncorrelated velocity goes to zero, which is consistent. When the particle inertia becomes very small where $\beta_p = \beta_f \to 1$ and $k_{fp} = k_{f@p} \to k_f$, the particle-phase dissipation tends to $\varepsilon_p \to \varepsilon_f$, as we can see from (D 1) and (D 2):

$$\frac{\mathrm{d}\varepsilon_f}{\mathrm{d}t} = (C_{\epsilon 1}\mathcal{P} - C_{\epsilon 2}\varepsilon_f)\frac{\varepsilon_f}{k_f} + C_3\frac{\varphi}{\tau_p}\left(\frac{k_{fp}}{k_{f@p}}\varepsilon_p - \beta_f\varepsilon_f\right), \tag{D 1}$$

$$\frac{\mathrm{d}\varepsilon_p}{\mathrm{d}t} = (C_{\epsilon 1}\mathcal{P} - C_{\epsilon 2}\varepsilon_p)\frac{\varepsilon_p}{k_p} + C_3\frac{1}{\tau_p}\left(\frac{k_{fp}}{k_{f@p}}\varepsilon_f - \beta_p\varepsilon_p\right). \tag{D 2}$$

Now we can check what happens to the stochastic equation for U_s. From the spatially homogeneous Lagrangian model, we can obtain

$$\mathrm{d}U_s + \varphi\mathrm{d}U_p = -\frac{1}{T_L}U_s\,\mathrm{d}t - \frac{\varphi}{T_{Lp}}U_p\,\mathrm{d}t + \sqrt{C_0\varepsilon_f}\,\mathrm{d}W_s + \varphi\sqrt{C_{0p}\varepsilon_p}\,\mathrm{d}W_p. \tag{D 3}$$

Now, when $\tau_p \to 0$, we can use one of the two equations to prove $\mathrm{d}U_s = \mathrm{d}U_p$, while the other two will give $\delta v_p \to 0$ and

$$\mathrm{d}U_s = -\frac{1}{T_L}U_s\,\mathrm{d}t + \frac{1}{(1+\varphi)}\sqrt{C_0\varepsilon_f}(\mathrm{d}W_s + \varphi\mathrm{d}W_p). \tag{D 4}$$

To obtain exactly the same equation as for one-way coupling, the white noise of the particle equation $\mathrm{d}W_p$ should be replaced, in this limit, by the one employed in the fluid velocity equation $\mathrm{d}W_s$. (In terms of the distribution function (i.e. weak convergence), the sum of two Wiener processes multiplied by constants is equivalent to a third Wiener process multiplied by the sum of the constants (Kloeden & Platen 1992).) If this is not done, when the transport equation of the second-order moments is evaluated, i.e. $\mathrm{d}\langle U_s^2\rangle$, there will be a spurious term $-2\varphi/(\varphi+1)^2 C_0\varepsilon_f$ due to the fact that the two noises are uncorrelated. In any case, this term goes consistently to zero when the mass fraction φ vanishes.

REFERENCES

Ahmed, A. M. & Elghobashi, S. 2000 On the mechanisms of modifying the structure of turbulent homogeneous shear flows by dispersed particles. *Phys. Fluids* **12** (11), 2906–2930.

Balachandar, S. & Eaton, J. K. 2010 Turbulent dispersed multiphase flow. *Annu. Rev. Fluid Mech.* **42**, 111–133.

Balkovsky, E., Falkovich, G. & Fouxon, A. 2001 Intermittent distribution of inertial particles in turbulent flows. *Phys. Rev. Lett.* **86** (13), 2790–2794.

Bosse, T., Kleiser, L. & Meiburg, E. 2006 Small particles in homogeneous turbulence: settling velocity enhancement by two-way coupling. *Phys. Fluids* **18** (2), 027102.

Brey, J. J., Dufty, J. W., Kim, C. S. & Santos, A. 1998 Hydrodynamics for granular flow at low density. *Phys. Rev.* E **58** (4), 4638.

https://doi.org/10.1017/jfm.2018.895 Published online by Cambridge University Press

BRILLIANTOV, N. V. & PÖSCHEL, T. 2010 *Kinetic Theory of Granular Gases*. Oxford University Press.

CAPECELATRO, J., DESJARDINS, O. & FOX, R. O. 2014 Numerical study of collisional particle dynamics in cluster-induced turbulence. *J. Fluid Mech.* **747**, R2.

CAPECELATRO, J., DESJARDINS, O. & FOX, R. O. 2015 On fluid–particle dynamics in fully developed cluster-induced turbulence. *J. Fluid Mech.* **780**, 578–635.

CAPECELATRO, J., DESJARDINS, O. & FOX, R. O. 2016*a* Strongly coupled fluid–particle flows in vertical channels. Part I. Reynolds-averaged two-phase turbulence statistics. *Phys. Fluids* **28** (3), 033306.

CAPECELATRO, J., DESJARDINS, O. & FOX, R. O. 2016*b* Strongly coupled fluid–particle flows in vertical channels. Part II. Turbulence modeling. *Phys. Fluids* **28** (3), 033307.

CAPECELATRO, J., DESJARDINS, O. & FOX, R. O. 2018 On the transition between turbulence regimes in particle-laden channel flows. *J. Fluid Mech.* **845**, 499–519.

CHIBBARO, S. & MINIER, J.-P. 2011 A note on the consistency of hybrid Eulerian/Lagrangian approach to multiphase flows. *Intl J. Multiphase Flow* **37** (3), 293–297.

CHOUIPPE, A. & UHLMANN, M. 2015 Forcing homogeneous turbulence in DNS of particulate flow with interface resolution and gravity. *Phys. Fluids* **27** (12), 123301.

CROWE, C. T., SCHWARZKOPF, J. D., SOMMERFELD, M. & TSUJI, Y. 2011 *Multiphase Flows With Droplets and Particles*. CRC Press.

DASGUPTA, S., JACKSON, R. & SUNDARESAN, S. 1994 Turbulent gas-particle flow in vertical risers. *AIChE J.* **40** (2), 215–228.

EATON, J. K. & FESSLER, J. R. 1994 Preferential concentration of particles by turbulence. *Intl J. Multiphase Flow* **20**, 169–209.

ELGHOBASHI, S. 1994 On predicting particle-laden turbulent flows. *Appl. Sci. Res.* **52** (4), 309–329.

ELGHOBASHI, S. & TRUESDELL, G. C. 1992 Direct simulation of particle dispersion in a decaying isotropic turbulence. *J. Fluid Mech.* **242**, 655–700.

ELGHOBASHI, S. E. & ABOU-ARAB, T. W. 1983 A two-equation turbulence model for two-phase flows. *Phys. Fluids* **26** (4), 931–938.

FERRANTE, A. & ELGHOBASHI, S. 2003 On the physical mechanisms of two-way coupling in particle-laden isotropic turbulence. *Phys. Fluids* **15** (2), 315–329.

FÉVRIER, P., SIMONIN, O. & SQUIRES, K. D. 2005 Partitioning of particle velocities in gas–solid turbulent flows into a continuous field and a spatially uncorrelated random distribution: theoretical formalism and numerical study. *J. Fluid Mech.* **533**, 1–46.

FORTERRE, Y. & POULIQUEN, O. 2008 Flows of dense granular media. *Annu. Rev. Fluid Mech.* **40**, 1–24.

FOX, R. O. 2003 *Computational Models for Turbulent Reacting Flows*. Cambridge University Press.

FOX, R. O. 2014 On multiphase turbulence models for collisional fluid–particle flows. *J. Fluid Mech.* **742**, 368–424.

GARDINER, C. W. 1990 *Handbook of Stochastic Methods for Physics, Chemistry and the Natural Sciences*, 2nd edn. Springer.

GATIGNOL, R. 1983 The Faxén formulae for a rigid particle in an unsteady non-uniform Stokes flow. *J. Méc. Théor. Appl.* **1** (2), 143–160.

GLASSER, B. J., SUNDARESAN, S. & KEVREKIDIS, I. G. 1998 From bubbles to clusters in fluidized beds. *Phys. Rev. Lett.* **81** (9), 1849.

GUALTIERI, P., BATTISTA, F. & CASCIOLA, C. M. 2017 Turbulence modulation in heavy-load suspensions of tiny particles. *Phys. Rev. Fluids* **2** (3), 034304.

GUAZZELLI, E. & MORRIS, J. F. 2011 *A Physical Introduction to Suspension Dynamics*. Cambridge University Press.

HINZE, J. O. 1975 *Turbulence*, 2nd edn. McGraw Hill.

INNOCENTI, A., MARCHIOLI, C. & CHIBBARO, S. 2016 Lagrangian filtered density function for LES-based stochastic modelling of turbulent particle-laden flows. *Phys. Fluids* **28** (11), 115106.

JENKINS, J. T. & SAVAGE, S. B. 1983 A theory for rapid flow of identical, smooth, nearly elastic, spherical particles. *J. Fluid Mech.* **130**, 187–202.

https://doi.org/10.1017/jfm.2018.895 Published online by Cambridge University Press

JENNY, P., ROEKAERTS, D. & BEISHUIZEN, N. 2012 Modeling of turbulent dilute spray combustion. *Prog. Energy Combust. Sci.* **38** (6), 846–887.

KLOEDEN, P. E. & PLATEN, E. 1992 *Numerical Solution of Stochastic Differential Equations*. Springer.

LAUNDER, B. E., REECE, G. JR & RODI, W. 1975 Progress in the development of a Reynolds-stress turbulence closure. *J. Fluid Mech.* **68** (03), 537–566.

MARCONI, U. M. B., PUGLISI, A., RONDONI, L. & VULPIANI, A. 2008 Fluctuation–dissipation: response theory in statistical physics. *Phys. Rep.* **461** (4–6), 111–195.

MAXEY, M. R. & RILEY, J. J. 1983 Equation of motion for a small rigid sphere in a nonuniform flow. *Phys. Fluids* **26** (4), 883–889.

MEHRABADI, M., HORWITZ, J. A. K., SUBRAMANIAM, S. & MANI, A. 2018 A direct comparison of particle-resolved and point-particle methods in decaying turbulence. *J. Fluid Mech.* **850**, 336–369.

MINIER, J.-P., CHIBBARO, S. & POPE, S. B. 2014 Guidelines for the formulation of Lagrangian stochastic models for particle simulations of single-phase and dispersed two-phase turbulent flows. *Phys. Fluids* **26** (11), 113303.

MINIER, J.-P. & PEIRANO, E. 2001 The pdf approach to turbulent polydispersed two-phase flows. *Phys. Rep.* **352**, 1–214.

MINIER, J-P., PEIRANO, E. & CHIBBARO, S. 2004 PDF model based on Langevin equation for polydispersed two-phase flows applied to a bluff body-body gas–solid flow. *Phys. Fluids* **16** (7), 2419.

MURADOGLU, M., POPE, S. B. & CAUGHEY, D. A. 2001 The hybrid method for the PDF equations of turbulent reactive flows: consistency conditions and correction algorithms. *J. Comput. Phys.* **172** (2), 841–878.

PEDLEY, T. J. & KESSLER, J. O. 1992 Hydrodynamic phenomena in suspensions of swimming microorganisms. *Annu. Rev. Fluid Mech.* **24** (1), 313–358.

PEIRANO, E., CHIBBARO, S., POZORSKI, J. & MINIER, J.-P. 2006 Mean-field/PDF numerical approach for polydispersed turbulent two-phase flows. *Prog. En. Comb. Sci.* **32** (3), 315–371.

PEIRANO, E. & MINIER, J.-P. 2002 Probabilistic formalism and hierarchy of models for polydispersed turbulent two-phase flows. *Phys. Rev.* E **65**, 046301.

PICANO, F., BREUGEM, W.-P. & BRANDT, L. 2015 Modulation of isotropic turbulence by particles of Taylor length-scale size. *J. Fluid Mech.* **650**, 5–55.

PICANO, F., BREUGEM, W.-P., MITRA, D. & BRANDT, L. 2013 Shear thickening in non-Brownian suspensions: an excluded volume effect. *Phys. Rev. Lett.* **111** (9), 098302.

POPE, S. B. 1985 PDF methods for turbulent reactive flows. *Prog. Energy Combust. Sci.* **11**, 119–192.

POPE, S. B. 1994 On the relationship between stochastic Lagrangian models of turbulence and second-moment closures. *Phys. Fluids* **6** (2), 973–985.

POPE, S. B. 2000 *Turbulent Flows*. Cambridge University Press.

POST, S. L. & ABRAHAM, J. 2002 Modeling the outcome of drop–drop collisions in diesel sprays. *Intl J. Multiphase Flow* **28** (6), 997–1019.

POZORSKI, J. & MINIER, J.-P. 1998 On the Lagrangian turbulent dispersion models based on the Langevin equation. *Intl J. Multiphase Flow* **24**, 913–945.

PUGLISI, A. 2014 *Transport and Fluctuations in Granular Fluids: From Boltzmann Equation to Hydrodynamics, Diffusion and Motor Effects*. Springer.

STICKEL, J. J. & POWELL, R. L. 2005 Fluid mechanics and rheology of dense suspensions. *Annu. Rev. Fluid Mech.* **37**, 129–149.

SUNDARAM, S. & COLLINS, L. R. 1999 A numerical study of the modulation of isotropic turbulence by suspended particles. *J. Fluid Mech.* **379**, 105–143.

TANAKA, M. 2017 Effect of gravity on the development of homogeneous shear turbulence laden with finite-size particles. *J. Turb.* **18** (12), 1144–1179.

TCHEN, C. M. 1947 Mean value and correlation functions connected with the motion of small particles suspended in a turbulent fluid. PhD Thesis, Delft.

TEN CATE, A., DERKSEN, J. J., PORTELA, L. M. & VAN DEN AKKER, H. E. A. 2004 Fully resolved simulations of colliding monodisperse spheres in forced isotropic turbulence. *J. Fluid Mech.* **519**, 233–271.

https://doi.org/10.1017/jfm.2018.895 Published online by Cambridge University Press

VIOLLET, P. L. & SIMONIN, O. 1994 Modelling dispersed two-phase flows: closure, validation and software development. *Appl. Mech. Rev.* **47** (6), S80–S84.

WANG, L. P. & STOCK, D. E. 1993 Dispersion of heavy particles by turbulent motion. *J. Atmos. Sci.* **50** (13), 1897–1913.

https://doi.org/10.1017/jfm.2018.895 Published online by Cambridge University Press